Investigating Ionic Liquid Chemical Structures for Applications in Whole Tumor Cell Vaccine Immunotherapy

Investigating Ionic Liquid Chemical Structures for Applications in Whole Tumor Cell Vaccine Immunotherapy

A thesis presented by

Garifalia “Litsa” Magdalini Kapsalis

to

the Faculty of the

Harvard John A. Paulson School of Engineering and Applied Sciences

in partial fulfillment of the requirements

for the Bachelor of Arts degree with honors in Engineering Sciences

Faculty Adviser: Prof. Samir Mitragotri

Harvard University

Cambridge, MA

March 31, 2024

Honor Code

In submitting this thesis to the Harvard John A. Paulson School of Engineering and Applied Sciences in partial fulfillment of the requirements for the degree with honors of Bachelor of Arts, I affirm my awareness of the standards of the Harvard College Honor Code.

Name: Garifalia Kapsalis

Signature: 

The Harvard College Honor Code Members of the Harvard College community commit themselves to producing academic work of integrity – that is, work that adheres to the scholarly and intellectual standards of accurate attribution of sources, appropriate collection and use of data, and transparent acknowledgement of the contribution of others to their ideas, discoveries, interpretations, and conclusions. Cheating on exams or problem sets, plagiarizing or misrepresenting the ideas or language of someone else as one's own, falsifying data, or any other instance of academic dishonesty violates the standards of our community, as well as the standards of the wider world of learning and affairs.

Acknowledgements

I am incredibly grateful to Prof. Samir Mitragotri for welcoming me into his laboratory. Since I took his Drug Delivery course two years ago, I have been fascinated with his research, and I have been honored with the opportunity to learn from his group. Prof. Mitragotri's advice and support have shaped my experience as an undergraduate and my future trajectory.

I am extremely indebted to Danika Rodrigues. Danika has mentored me since welcoming me to the lab and has been a constant source of inspiration and guidance. Working with Danika has fundamentally impacted my life. Through her patience and kindness, I not only learned *how* to research, but I also developed a profound passion for science and the confidence to pursue a PhD upon graduation. I am so grateful for the many hours of training, troubleshooting, editing, and advice that she has given me. She is a talented mentor and a genuine friend, and I am so fortunate to have been able to work with her for the past four semesters.

I have immense gratitude for everyone in the lab. I owe many thanks to Claudia Stearns for her kindness and support and to Dr. Bijay Singh for helping me and making me feel welcome. Many thanks to the group's post docs, for your encouragement and patience with all of my questions: Dr. Mete Erdi, Dr. Rick Liao, Dr. Kolade Adebowale, Dr. Charles Park, Dr. Vinny Suja, Dr. Anujan Rames, and Dr. Shuyang Zhang. Thank you also to the lab's graduate students (and recent graduates) -- Morgan Goetz, Morgan Janes, Neha Kapate, Ninad Kumbhojkar, Supriya Prakesh, Shrini Acharya, Griff Bibbey, Maithili Joshi, Malini Mukherji, and Suyog Shaha – for your advice, kindness, and warmth.

From my very first semester of college, Dr. Linsey Moyer, my Bioengineering advisor and ES 53 instructor, has constantly helped me and enabled my passion for this area of study. From countless meetings discussing course requirements, to helping me connect with research opportunities throughout college, to talking through my thesis plans, Dr. Moyer has been a constant support system. Because of her, I felt that I could study engineering here. I cannot thank Dr. Moyer enough.

Thank you to my very many other academic and research advisors and mentors: Prof. Sam Stupp and Dr. Tom Cotey at Northwestern who patiently trained and supported me during my first ever lab experience; Dr. Dave Mooney, Dr. Irene de Lázaro, and Mason Dacus, for their impactful mentorship that deepened my fascination for drug delivery and sparked my interest in immunoengineering; Prof. Joanna Aizenberg, my materials science professor who believed in me; and Dean Frank Doyle, for his incredibly generous advising.

I could not imagine my life without my incredible friends and support system. Thank you to each and every one of them who supported me through all the difficult days and for creating a home away from home. A special thank you to my roommates – Gabby Grant, Julia Gavel, and Sophia Charles – whose unconditional kindness and encouragement made my undergraduate experience the best time of my life so far. I would not be where I am today without my friends at home, especially Kiera Burns: thank you for our unbreakable, lifelong friendship.

I owe everything to my loving family whose constant support and confidence in my abilities allowed me to flourish. This thesis is dedicated to them. To Mama and Baba: I am so proud to be your daughter, and I am forever grateful for your lessons, encouragement, and love. To my sister, Madeleine, and my brother, Kosta, for being there for me no matter what time of day or night, and for always rooting for me. Thank you to my grandparents, who are my greatest inspirations and sources of strength and identity. I strive to become like them.

Above all, I am grateful to God.

Attribution of Work

This work was conducted under the guidance and supervision of Professor Samir Mitragotri, Hiller Professor of Bioengineering and Hansjorg Wyss Professor of Biologically Inspired Engineering.

Dr. Linsey Moyer, Assistant Director of Undergraduate Studies in Biomedical Engineering, helped me helped me with thesis logistics and helped me ensure I met the concentration's guidelines for my senior thesis.

I conducted experiments in the thesis alongside Danika Rodrigues, a doctoral candidate in Bioengineering at the Harvard School of Engineering and Applied Sciences.

The synthesis and IC50 determination (Table 2; Figure 6A) of choline hexanoate, choline heptanoate, and choline decanoate, three ionic liquids used as reagents and treatments in my Panel 1, were conducted by Danika Rodrigues prior to my joining the lab. Danika Rodrigues helped capture NMR spectra of newly synthesized ILs (Figure 5), helped set up and run the Panel 1 Necroptosis Determination Assay (Figure 10), and helped run the Panel 1 Necroptosis Determination Assay (Figure 11).

I received course credit for my research in the Mitragotri Lab during Fall 2023 through ENG-SCI 91r. I received funding for my research through Harvard College Research Program Grants in Spring 2023 and Spring 2024.

Abstract

Whole tumor cell vaccines are an emerging immunotherapy strategy whereby tumor cells are inactivated and modulated *ex vivo* prior to injection back into a patient to deliver a library of antigens for the body's immune system to recognize and target. Currently, irradiation is the most common method of *ex vivo* induction of cell death in tumor cell vaccines. However, irradiation has limitations, especially insufficient tumor immunogenicity. In this study, we explored ionic liquids (ILs) as alternatives in the preparation of whole tumor cell vaccines.

Here, we aimed to create a tunable library of ILs for whole tumor cell vaccines by determining the impact of IL anion length, branching, and unsaturation on 4T1 murine mammary cancer cells. We examined the impact of IL anion structure on cell cytotoxicity, cell death pathways, immunogenicity of cell death, and autophagy activation.

We determined that IL-induced cytotoxicity increases with anion carbon chain length and with concentration, and decreases by adding branched methyl, ethyl groups, and double bonds (with constant carbon chain length) in the anion structure. Among all ILs, apoptosis appeared as the primary mechanism of cell death, though the stage of apoptotic activity was tunable. Furthermore, anion branching and unsaturation decreases exposure of calreticulin. ILs were shown to induce ATP release in a concentration-dependent manner, though autophagy was not observed to be induced significantly.

This work has provided further characterization of the biological interface of ILs in activating whole tumor cell vaccines and has demonstrated their tunable ability to induce immunogenic activity in cancer.

Table of Contents

List of Figures

List of Tables

1. Introduction

1.1 Significance

Solid tumors account for roughly ninety percent of all cancer-related deaths [1]. These tumors pose significant therapeutic hurdles and are often resistant to conventional treatments, such as chemotherapy and radiation therapy [2]. Immunotherapy has garnered significant interest for the treatment of solid tumors by as it aims to engage a patient's immune system to fight the cancer from within. This class of therapies, including immune checkpoint inhibitors (ICI), monoclonal antibodies (mAb), chimeric antigen receptor T cell (CAR-T), and cancer vaccines, has seen incremental successes in preclinical and clinical studies, though its effectiveness can be hindered by various immune suppression mechanisms activated by cancer [3]. Across immunotherapy – and all forms of cancer treatment – there is a critical need for strategies with increased and optimized immunogenicity. One such approach is through activating immunogenic cell death (ICD) in tumors, which prompts anti-cancer immune response [4], [5], [6]. However, challenges remain in activating ICD while minimizing cytotoxicity on non-cancerous tissue, which causes harmful side effects [4].

This present study explores the application of ionic liquids (IL) in whole tumor vaccine immunotherapy and seeks to understand how the modulation of these compounds' chemical structures may impact the aforementioned factors contributing to the efficacy of solid tumor treatment. Here, we investigate how the IL anion structures may calibrate their ability to induce cytotoxicity, ICD, and various cell death pathways in 4T1 cells, an *in vitro* murine model for triple negative breast cancer, a form of aggressive solid tumor. Ultimately, we aim to optimize IL applications in whole tumor cell vaccine immunotherapy.

1.2 Motivation

Preliminary work within the Mitragotri Lab has suggested the potential utility of ionic liquids (ILs) to induce *ex vivo* cell inactivation and death of 4T1 cells for use in whole tumor cell vaccines. Co-cultures were conducted of 4T1 cells treated with a panel of choline based ILs along with dendritic cells (DCs). In this study, a panel of ILs containing various lengths of carbon chains were screened, and it was found that treatment of 4T1 cells with certain ILs enhanced the phagocytosis of tumor cells by DCs. This effect was most apparent with the IL choline octanoate (an IL containing eight carbons) and was shown to be dose dependent. Within this IL screen, choline octanoate also caused upregulation in DC activation markers, namely CD80, CD86, and CD40. These results suggest that ILs could be a promising method of inducing immunogenic cell death (ICD) for whole tumor cell vaccine preparation.

This thesis aims to understand the effect of IL structure on cells upon treatment for application in whole tumor cell vaccine preparation. Here, we investigate the mechanisms by which ILs act to induce ICD as well as the tunability of their structure for whole tumor cell vaccine applications. By doing so, this research seeks to contribute to the broader field of therapeutic cancer vaccine development.

Here, we will look at a two panel of ILs with various anion structure. The first panel includes ILs with anions of various carbon chain lengths. Since choline octanoate, an IL with an eight-carbon anion chain, was primarily successful in increasing tumor cell uptake by dendritic cells (DCs),

we will also look at a second panel including various isomers of eight-carbon anion chains by modifying structure with branching and unsaturation.

With each panel, we examine cytotoxicity, cell death pathways and immunogenic markers. Immunogenicity of cell death, especially regulated cell death, often cannot be predicted based on the pathways that lead up to it. Thus, it is helpful to measure cytokines, chemokines, and other damage-associated molecular patterns (DAMPs) that are indicative of immunogenicity and understand if and how modulating IL chemical structure is able to tune immunogenicity [7]. We measured such chemical signals released by 4T1 cells treated by two panels of ILs. Specifically, we examined biomarkers that are common to irradiation, since we are exploring whether ILs can be used as a substitute for irradiation in preclinical whole tumor cell vaccine studies [8]

Panel 1 included four different ILs of increasing anion chain lengths (choline hexanoate, choline heptanoate, choline octanoate, and choline decanoate). Panel 2 included choline octanoate and three of its isomers (choline 2,2 dimethylhexanoate, choline 2-ethylhexanoate and choline trans-2-octenoate).

1.3 Hypothesis

We hypothesized that ILs with longer anion chain lengths will be increasing cytotoxicity, due to increased lipophilicity. Based on previous literature and because previous work in our lab found that choline-based ionic liquids increased phagocytic uptake of treated 4T1 cells by DC, we hypothesized that IL-induced cell death is immunogenic [9]. In particular, immunogenic apoptosis has been reported to induce phagocytic uptake of tumor cells in by prompted damage-

associated molecular pattern (DAMP) emission [10]. As such, we hypothesized that immunogenic apoptosis will be the primary pathway of cell death [11].

Moreover, we hypothesized that because branched molecules and unsaturated molecules are less lipophilic than straight-chain molecules, these isomers of choline octanoate will be less cytotoxic and result in less pronounced release and exposure of immunogenic markers, namely ATP and calreticulin, when treating 4T1 cells. However, despite varying lipophilicity and hypothesized resulting changing cytotoxic activity, the way in which the branched and unsaturated anions interact with the cell will be fundamentally similar to the straight-chain choline octanoate, so we again predicted that apoptosis will be the primary mechanism of cell death. Finally, because apoptosis can lead to triggered autophagy in some ICD cases, we hypothesized that IL treatment trigger autophagy [12].

1.4 Specific Aims

In order to test these hypotheses, the following specific aims guided our study:

1. Determine the effect of anion structure on cytotoxicity among choline-based ILs
2. Compare cell death pathways induced by various IL anion structures
    1. Evaluate the cell death pathway of a panel of four ILs of varying anion carbon chain lengths, including choline octanoate, as well as a panel of four choline octanoate isomers. Employ flow-cytometry-based and colorimetric-based techniques that assay markers for apoptosis, necroptosis, and necrosis
3. Investigate the effect of IL anion structure on immunogenicity of cell death

1. Use flow cytometry and luminescence-based assays to understand immunogenic marker presence by probing for and calreticulin exposure and ATP release; investigate role of autophagy in IL-induced cell death

2 Background and Literature Review

2.1 Challenges in immunotherapy for solid tumors

Immunotherapy is a class of therapies by which the immune system is boosted in order to identify and eliminate cancerous cells [13]. The first documented immunotherapy was reported in 1891 when American surgeon William Coley used bacterial combinations to elicit an immune response. The therapy's mechanism of action was not understood at the time, but it was observed that the responses to infection were associated with the regression of patients' tumors [3]. Now, cancer immunotherapy offers new avenues for treatment of cancer, including immune checkpoint inhibitors (ICI), monoclonal antibodies (mAb), chimeric antigen receptor T cell (CAR-T), and cancer vaccines [3]. In the past, the standard of care for cancer treatment has typically been surgery, chemotherapy, or radiation, with many solid tumor patients requiring a combination [14]. Chemotherapy bears significant side effects, such as hair loss, sterility, damage to the heart, liver, and kidneys, and accelerated aging [15], [16].

While various forms of immunotherapy have seen approvals in hematological cancers, success in immunotherapy for solid tumors is more difficult to come by [3]. Solid tumors have a highly immunosuppressive tumor microenvironment (TME). The tumor extracellular matrix often has high numbers of growth factor-synthesizing fibroblasts, and its stromal composition leads to high

pressure of the interstitial fluid, which makes it difficult for macromolecules to penetrate [17]. Nevertheless, several ICI immunotherapies targeting solid tumors have been approved [18].

2.2 Challenges in immunotherapy against Triple Negative Breast Cancer

Triple negative breast cancer (TNBC), a solid tumor cancer wherein the progesterone receptor, HER2/neu and estrogen receptor are absent, is one of the most aggressive types of solid tumors [19]. TNBC, which affects 10-20% of breast cancer patients, is highly heterogeneous [20]. Moreover, the TME inhibits cell apoptosis, which can lead to hypoxia and oxidative stress, resulting in chemotherapy resistance [21]. Various immunotherapy strategies have been explored for the treatment of TNBC. ICI treatment, such as anti-PD-1/PD-L1 antibody treatment , has demonstrated anti-tumor activity in patients, and anti-CTLA-4 therapy, though it is not yet approved, may have utility in blocking axillary lymph node metastasis and in reducing breast tumors. ICIs have been explored as monotherapies, combination therapies with each other, and in combination with gene therapies, radiotherapy, chemotherapy, and other novel therapies [21]. Additionally, unmethylated cytosine-phosphorothioate-guanine (CpG) oligodeoxynucleotides (CpG), especially category B (CpG-B) have been found to significantly reduce tumor growth as a monotherapy or in combination with PD-1 blockade [21], [22]. CpG is a toll-like receptor 9 (TLR9) agonist, which activates T and B cells and increases release of interferon (IFN) α and β by stimulating dendritic cells [22].

Other forms of immunotherapies are being explored for applications against TNBC. As of Jan 2023, sixteen different cancer vaccines against TNBC were in clinical trials [23]. Vaccines are generally either peptide-based, cell-based, or nucleic acid-based [23]. They either target tumor-

associated antigens (TAA), which are markers expressed in normal cells and tumor cells, or tumor-specific antigens (TSAs), which are only expressed in cancer cells, by activating an immune response against these tumor markers. Neoantigens are markers expressed on an individual's specific TAAs; these make up around a quarter of cancer vaccines in trials for TNBC.

In 2015, a Phase I clinical trial of a personalized synthetic long peptide vaccine to treat TNBC began. However, this study was withdrawn in 2022 with no reason provided [24]. In 2020, a Phase I clinical trial of neoantigen DNA vaccine was run [25]. This vaccine directly administered recombinant DNA that encodes for multiple patient-specific neoantigens. The study reported that in the 18 patients in which the treatment was administered, the treatment was generally well-tolerated, and it was suggested that significant neoantigen-specific responses were observed. The study also suggests that while clinical response was not formally assessed, patents treated with the neoantigen vaccine displayed improved progression-free survival compared to "historical controls" [26]. In 2020, a Phase I clinical trial (NCT02316457) of a personalized neoantigen mRNA vaccine induced T-cell responses in TNBC patients [27], [28].

2.2.1 Triple Negative Breast Cancer Model

The 4T1 murine breast cancer cell line is a transplantable mammary tumor model which is able to grow as an adherent culture or in BALB/c mice [29]. It was isolated from a mammary BALB/c 410.4 tumor [30]. It is a highly invasive and metastatic tumor line, and similarly to human breast cancer, it can spontaneously grow in secondary tumors in the lymph nodes, lungs, brain, and other organs. It is often used in preclinical immunotherapy studies, especially those

aiming to activate CD4+ and CD8+ T cells and including cell-based vaccines. 4T1 cells are poorly immunogenic, which further resembles human breast tumors [31].

2.3 Advances in whole tumor cell vaccines

Whole tumor cell vaccines for cancer treatment are an emerging immunotherapy strategy whereby tumor cells are inactivated and modulated *ex vivo* prior to injection back into the patient to deliver a library of antigens for the body's immune system to recognize and target (Figure 1). This strategy has the potential to mitigate some of the challenges in treating highly heterogeneous solid tumors, such as TNBC, because tumor specific-antigens do not need to be identified prior to treatment. Currently, there are no approved whole tumor vaccine therapies, although there is activity in Phase I and Phase II clinical trials [32]. Often, these whole tumor cell vaccines are in combination with other drug agents or adjuvants.

Various studies have shown that tumor lysates, in combination with other agents, could activate immune cells against TNBC. For example, hypochlorous acid-oxidized lysates with CpG increased activation of DCs [20], [33] In another study, irradiated whole tumor cells and subsequent exposure to an oncolytic virus-infected cell vaccine also increased DC recruitment and activation [20].

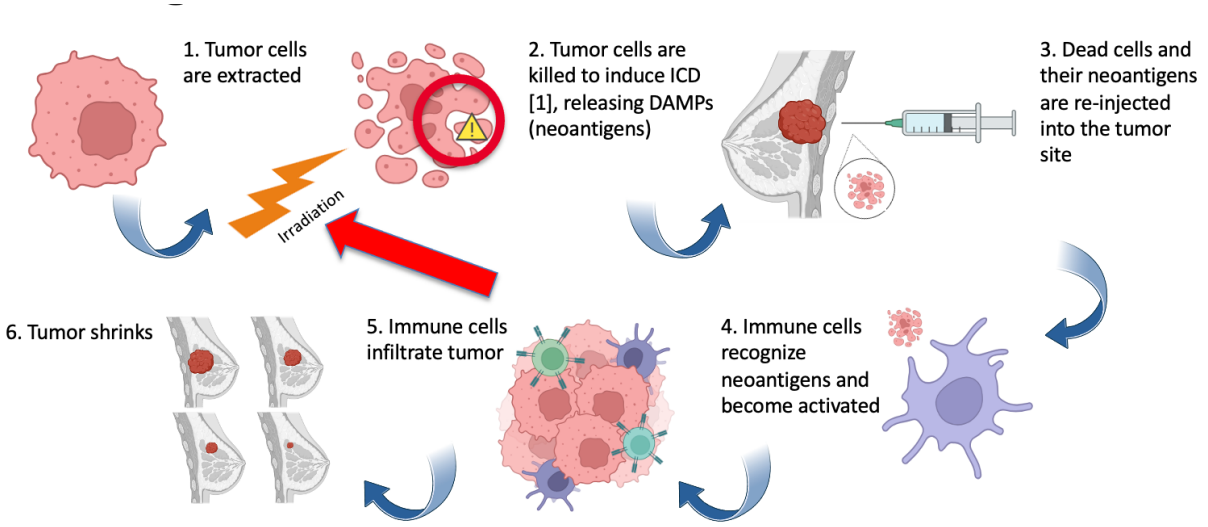

Figure 1. General concept of whole tumor cell vaccine immunotherapy. *Created with BioRender.com.*

2.4 Immunogenic markers

Immunogenicity of whole tumor cell vaccines is essential for the activation of T cell responses against tumors [33]. Various biomarkers, such as calreticulin (CRT), adenosine triphosphate (ATP), high mobility group protein (HMGB1), can be used to measure immunogenic response to a substance or therapy [33]. CRT binds to calcium ions in the endoplasmic reticulum (ER) and translocates to the surface of tumor cells [34]. CRT induces the DC and macrophage phagocytosis of dying cancer cells, and factors such as HMGB1 and ATP are secreted to induce antigen processing and DC maturation [32], [33], [35]. These molecules are also recognized by TLRs on antigen-presenting cells, which activates immune cells, such as DCs [33].

Currently, in whole tumor cell vaccine processes, irradiation is the most common method of *ex vivo* induction of cell death in tumor cell vaccines. However, irradiation has limitations, especially insufficient immunogenicity of tumor cells. Finding alternatives to irradiation is an

active area of research [36], [37], [38]. Other common methods by which cell death is induced in whole tumor cell vaccines are hypochlorous acid treatment, which increases immunogenicity via oxidation, freeze-thaw, which results in cellular fragmentation and necrotic cell death, and hyperthermia (heat-killing) [34]. Various strategies for inducing *ex vivo* cell death result in varying levels of immunogenicity. *Here, we seek to investigate a potential alternative to irradiation for inducing ex vivo cell death in whole tumor cell vaccines.*

2.5 Immunogenic cell death in whole tumor cell vaccines

Immunogenic cell death (ICD) is cell death that triggers an immune response against "dead-cell antigens" [39]. Importantly, these markers of ICD, such as CRT, ATP, and HMGB1 have been shown to be significantly induced by anti-cancer agents, such as cardiac glycosides, that extend the survival of breast cancer patients who were treated with non-anthracycline agents [8].

In whole tumor cell vaccine preparation, immunogenic cell death is crucial for providing a library of neoantigens against which the immune system can be inoculated. Kroemer et al. defines two main criteria of ICD for cancer vaccine applications. First, cells that undergo ICD and are administered to a mouse model must protect the animal against future challenges with the same type of live tumor cells. Secondly, *in vivo* ICD must recruit both innate and adaptive immune cells to the location of the tumor and act to suppress its growth [39]. *Because ICD is crucial for efficacy of tumor-reduction in whole tumor cell vaccines, this thesis seeks to understand and measure the immunogenicity of ex vivo cell inactivation and death induced by ionic liquids.*

2.6 Cell death pathways

Different *ex vivo* cell death inducing methods also activate differing cell death pathways [34]. Cell death pathways are often classified as regulated/programmed or un-regulated cell death. In regulated cell death, the cell dies through internal molecular machinery in response to cues [40], [41]. In unregulated cell death, the cell is unable to survive due to stress.

2.6.1 Apoptosis

Apoptosis is a form of regulated cell death (RCD) that plays a key role in post-embryonic development and tissue homeostasis. Cell damage initiates apoptosis via caspase-dependent pathways that induce DNA fragmentation and the deterioration of proteins in the nucleus [42]. Morphologically, it is characterized by blebbing and contraction of the cell membrane [43]. It can be induced either intrinsically, via sensing of intracellular damage, or extrinsically, via binding of extracellular "death ligands" [44]. Apoptosis typically occurs during organism development, cell turnover, or via drug compounds [44]. During its process, it degrades proteins and chromosomal DNA, forms apoptotic bodies, and is uptaken by phagocytes [44]. Inhibition of apoptosis can be implicated in oncogenesis and a host of other disorders [45]. Previously, it was believed that apoptosis is non-immunogenic, but this has been determined to be an oversimplification; its release of various damage associated molecular patterns (DAMPs), such as CRT and HMGB1, contributes to its immunogenicity [46].

At the early stages of apoptosis, phosphatidylserine (PS) is translocated from the inner plasma membrane to being exposed on the outer [47]. One method of detecting apoptosis is by treating with fluorescently labelled Annexin V; PS binds Annexin V, a phospholipid-binding protein that

is a common indicator for PS exposure. Annexin V is commonly used alongside propidium iodide (PI), which is an indicator of a damaged cell membrane. The Annexin V/PI assay is widely used to detect and identify the stage of apoptosis. Necrotic cells, similar to apoptotic cells, expose PS on their cell membrane. However, unlike apoptotic cells, necrotic cells have a ruptured cell membrane, so they are seen to be PI positive [47]. Later studies, however, have shown that cells that are positive for both Annexin V and PI can also exhibit late apoptosis [48]. Thus, when cells stain Annexin V+/PI+, the presence of necrosis compared to late apoptosis can be probed with necrosis determination assays, such as a lactate dehydrogenase assay.

2.6.2 Necrosis

Necrosis is a form of unregulated cell death induced by injury, and it is often prompted by shock, such as radiation, heat, hypoxia, or inflammation [42]. During this process, the cell membrane ruptures, and its contents spill out. One way to identify necrosis is through the detection of lactate dehydrogenase (LDH). This cytoplasmic enzyme is leaked extracellularly when the cell membrane breaks during necrosis. To detect LDH, treating a culture with a tetrazolium salt can react with NADH to form a byproduct that can be observed by measuring colorimetric absorbance [49].

2.6.3 Necroptosis

Necroptosis is a form of program cell death that imitates elements of both apoptosis and necrosis [50]. Like necrosis, it induces the release of cytokines and chemokines, and is morphologically marked by swelling and bursting of the plasma membrane. Similar to apoptosis, necroptosis is initiated by cellular signaling, such as by toll-like and interferon receptors [50], [51]. Crucially,

unlike in apoptosis, necroptosis requires Receptor-Interacting Protein Kinase 3 (RIP3), along with Receptor-Interacting Protein Kinase 1 (RIP1) to form part of the necrosome complex, which activates a cascade that results in necroptotic processes [52]; RIP3 can transition a cell from apoptosis to necroptosis [53]. One way in which necroptotic activity can be identified is by detection of RIP3 expression. This is often assayed in combination with caspase-3 (Casp-3); since necroptosis is a caspase-independent process, the expression of RIP3 and the absence of Casp-3 expression can indicate necroptosis [54]. However, since apoptosis is caspase dependent but often independent of RIP3, RIP3 -/ Casp-3+ can indicate apoptosis. Necroptosis is inhibited by necrostatin-1 by blocking RIP1 [50], and apoptosis can be inhibited by treatment with the caspase inhibitor carbobenzoxy-valyl-alanyl-aspartyl-[O-methyl]-fluoromethylketone (zVAD - FMK) [55], both of which can be used as controls for a RIP3/Casp-3 assay [54].

2.7 Autophagy

Autophagy is a mechanism by which cellular components are separated into lysosomes, where they are either degraded or recycled [42]. During autophagy, intracellular double membranes called pre-autophagosomes form during membrane expansion [56]. These vesicles engulf their cargo and then fuse to form a developed compartment called an autophagosome and then deliver their cargo to the lysosome via membrane fusion, forming an autophagolysosome. Here, the cargo is degraded, and the degradants are re-exported to the cytoplasm [56]. One way to detect autophagy is by staining autophagic compartments and quantifying signal via flow cytometry [57].

Autophagy can either be pro-death or pro-survival, and its crosstalk with apoptosis is involved in various functions and pathologies, such as homeostasis or conversely, cancer [44]. In healthy cells, autophagy and apoptosis both suppress tumors, as the former degrades oncogenic molecules and the latter prevents tumor cell survival [58]. However, when either autophagy or apoptosis are defective, this can cause cancer. Defective apoptosis leads to lack of insufficient death of cancer cells. Among other consequences, impaired autophagy can contribute to cancer cell resistance and survival in environments where they experience hypoxia or low amounts of nutrition [58]. Further, in tumor cells with defective apoptosis machinery, autophagy may activate to induce cell death, so when it is impaired, it could lead to tumor growth [59].

Autophagy can be consequential for immunogenic cell death. When autophagy is inhibited, dying cells still expose CRT and release HMGB1, but their ATP secretion is blocked [60]. Michaud et al. found that inhibiting extracellular ATP-degrading enzymes can restore immune cell recruitment [60]. Therefore, it was found that autophagy can lead to immunogenic release of ATP in cell death, specifically in apoptosis. In autophagy-deficient cancer cells, CRT was exposed in similar amounts to autophagy-competent cancer cells. Moreover, in murine colorectal carcinoma cells, both autophagy-competent and autophagy-incompetent cells responded to the chemotherapeutic agent mitoxantrone with apoptosis. However, autophagy-competent cells were able to induce antitumor immunity while autophagy-deficient cells were unable to could not prime T cells *in vivo* [60].

Despite the aforementioned mechanisms by which autophagy can aid in tumor defense, autophagy has also been observed to be involved in processes that can propagate tumor

formation. For example, it has been found to be used as a protective mechanism by cancer cells, and it has also been shown to promote angiogenesis within tumors as well as metastasis [12], [61]. The interplay between autophagy, ATP, ICD, and tumor growth is complex, and thus it is important to understand how potential immunotherapy strategies modulate these processes.

In this thesis, we will investigate the cell death pathways induced by *ex vivo* treatment of cells by ionic liquid in order to understand the mechanisms by which ionic liquids interact with cells.

2.8 Ionic Liquids

Ionic liquids (ILs) are bulky, asymmetric salts made up of cations and anions with melting points below 100°C. They are of growing interest for a variety of applications, including within biomedicine [62], [63]. ILs have been useful in the solubilization of drugs and in formulating drugs for transdermal drug delivery [63]. Ali et al. utilized an ionic liquid formulated consisting of choline and oelic acid to increase solubility of active pharmaceutical ingredients, such as celecoxib, acyclovir, and methotrexate by more than twenty times the solubility of water [63], [64].

2.8.1 Ionic Liquids as Therapeutics

In addition to formulation, ILs have shown promise as therapeutic or active pharmaceutical components. Previous work from the Mitrogotri lab found that an orally delivered choline and geranic acid-based IL (CAGE) can solubilize fat model-molecules to reduce fat absorption in a

rat model. CAGE did not appear to be toxic to the rats, nor cause adverse events, and thus could have applications in obesity treatment [65].

Among other applications, ILs have been of interest in cancer treatment [9]. Previous work has suggested that ILs have tumor-specific cytotoxicity [66]. For example, an imidazolium-based IL showed selective toxicity to bladder cancer cells in a mouse model, not affecting nearby healthy cells [67]. Moreover, choline and geranic acid based ILs have been observed to induce DC maturation during tumor ablation in a pancreatic carcinoma model [68] and sensitize tumors to chemotherapy agents in a hepatocellular carcinoma model [69].

2.8.2 Ionic Liquid Cell Cytotoxicity

Many previous works on IL toxicity have aimed to elucidate their potential danger when utilized industrially, especially as a potentially environmentally-friendly substitute for organic solvents [66], [70]. Previously, it has been demonstrated that the cytotoxicity of imidazolium-based ILs has mostly depended on their cation concentration and carbon chain length [11]. Musiał et al., however, further examined anion effect on cytotoxicity and found that more lipophilic anions are able to interact with hydrophobic membranes and protein domains, thus disrupting cell physiology [71]. Petkovic et al. screened a panel of cholinium alkanoates with different anion chain lengths and branching on four fungal isolates and found that toxicity increased with anion chain length and decreased with branching, correlating with the decrease in lipophilicity of branched ions compared to unbranched ions [72]. Moreover, Chism et al. reported that saturated ILs are more bactericidal than unsaturated ILs [73]. However, it has been reported that the same IL may have different effects on the different cell lines [71].

2.8.3 IL-induced Cell Death Pathways and Cytotoxic Mechanisms

Various mechanisms of cytotoxicity have been proposed among ILs compounds treating different cell types. Li et al. suggested that imidazolium-based ILs induced apoptosis in rat pheochromocytoma cells [11], a rare tumor that begins in the adrenal medulla [74]. Treated cells demonstrated by caspase-3 activity, excessive reactive oxygen species (ROS) levels, and other apoptotic markers [11].

Gal et al. examined six ILs each with cation types and cation side-chain structures [70]. The anion of five of the six ILs studied was chloride, and the other used was bromide. IL-cell interaction was studied using U937 monocytic cells, a human cell line. Results demonstrated a large variation of IL-cell interactions. The extent to which ILs bound and disrupted the cell lipid bilayer varied between ILs, but all ILs studied demonstrated some form of membrane interactions, despite a wide range of cytotoxic activity, supporting the tunability of IL-cell interacting mechanisms [70].

Molecular dynamics studies have suggested that ILs are able to insert themselves into cell membranes, leading to pores or rupture [75], [76]. Moreover, ILs can damage the membrane structure of HeLa cells by increasing oxidative stress, altering cell morphology and impacting protein structure [76]. Again, lipophilicity of ILs has been widely correlated with cytotoxicity, corroborating the role that membrane interactions and disruptions play in their toxic effects [70], [77], [78].

3. Materials and Methods

3.1 Ionic Liquids

This study included two separate libraries of ionic liquids. The multi chain-length library (panel 1) included choline propanoate, choline hexanoate, choline heptanoate, choline octanoate, and choline decanoate. With the exception of choline octanoate, these ILs were synthesized from previous work within our lab. They were all used for the current study.

The choline octanoate isomer library (panel 2) included choline octanoate, choline 2,2 dimethylhexanoate, choline 2-ethylhexanoate, and choline trans-2-octenoate. These ILs were all both synthesized and used within this current study.

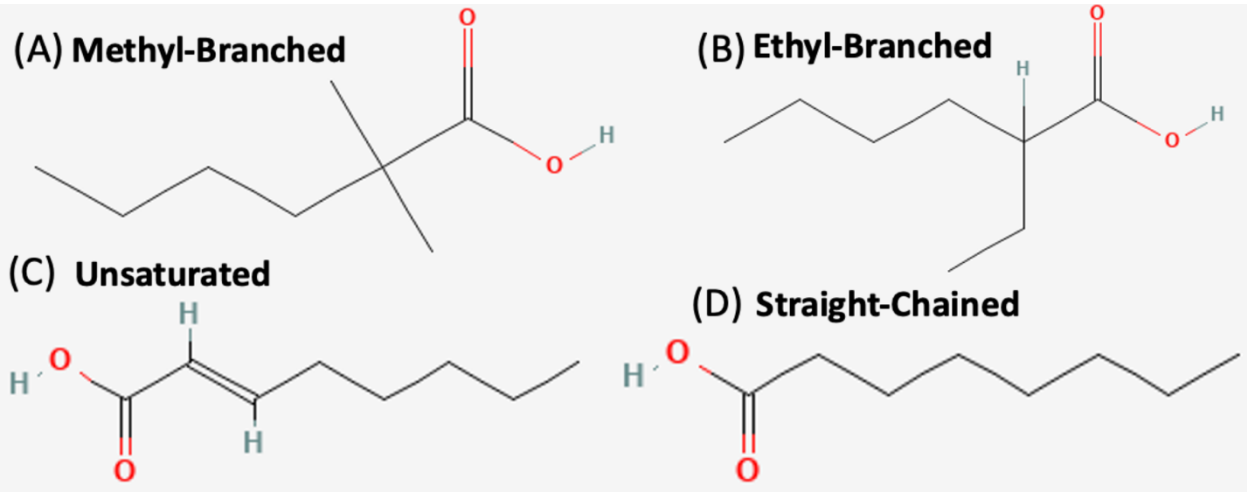

Figure 2. Chemical structures of acids utilized in ionic liquid synthesis. (A) 2,2-dimethylhexanoic acid, (B) 2-ethylhexanoic acid, (C) trans-2-octenoic acid and (D) octanoic acid *Adapted from PubChem - National Library of Medicine* [79], [80], [81], [82].

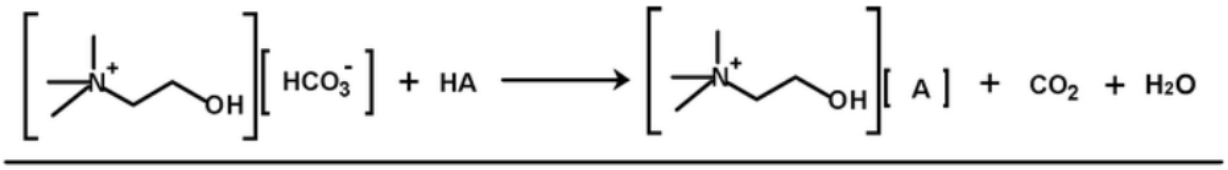

Figure 3. Depiction of chemical route for obtaining the choline alcoate ionic liquids. *From Petkovic et al. 2010.* [72]

3.1.1 Ionic Liquid Synthesis

We synthesized four ionic liquids at a 1:1 anion to cation ratio (Figure 2). Choline octanoate was synthesized with choline bicarbonate and octanoic acid. Choline 2,2-dimethylhexanoate was synthesized with choline bicarbonate and 2,2-dimethylhexanoic acid. Choline 2-ethylhexanoate was synthesized with choline bicarbonate and 2-ethylhexanoic acid. Choline trans-2-octenoate synthesis was attempted from choline bicarbonate and trans-2-octenoic acid.

The following reagents were used: Choline bicarbonate (Sigma Aldfrich, 80% in water), 2,2 Dimethylhexanoic Acid (LabPro, purity >= 98.0%), 2-Ethylhexanoic Acid (Lab Pro, purity >= 99.0%), trans-2-Octenoic Acid, (Lab Pro, purity >=98.0%), Octanoic Acid (Sigma-Aldrich, purity >= 99.0%)

We carried out the reactions, dropwise between each pair of components at 40°C overnight. The solution was then transferred to a rotary evaporator for several hours and finally put in a vacuum oven at 60°C for 48 h to remove residual water. The IL was collected in a glass vial. Compounds were synthesized according to the methods outlined by Petkovic et al. [72] The synthesis of choline trans-2-octenoate included minor modifications. After 48 hours in the vacuum oven, we

repeated its rotary evaporation and subsequent 48h in a vacuum oven at 60°C for 48 h before collecting in a glass vial.

3.1.2 Ionic Liquid NMR

We assessed synthesis of each ionic liquid using NMR spectroscopy. The NMR spectra were collected using a 400-MHz Bruker AVANCE NEO 400 (N400) instrument.

3.2 4T1 Cells

3.2.1 Media

The complete culture medium is Roswell Park Memorial Institute (RPMI) 1640 with 10% Fetal Bovine Serum (FBS) and 1% Penicillin-Streptomycin (P/S).

3.2.2 Cell Preparation From Stock Supply

A vial of 4T1 cells frozen at -80 ℃ is thawed at 37 ℃. The contents are then washed in media and then transferred and seeded in a flask of warm media.

3.2.3 Subculture

4T1 cells are subcultured in T-75 flasks every 2-3 days when cells are around 80% confluent. First, media is removed from the T-75 flask and cells are washed with 10 mL of DPBS. Then, 2 mL of Trypsin-Ethylenediaminetetraacetic acid (Trypsin-EDTA) solution is added in order to unadhere cells. Trypsin-treated cells are incubated at 37°C for 5 - 10 minutes. The flask is examined with an inverted microscope to check that cells are disbursed and no longer adhered. Then, 8 mL of complete medium is added to quench the trypsin reaction, and cells are

centrifuged at 150 g for 5 minutes. The cells are counted with a 1:4 dilution in Trypan Blue on a Bulldog Bio 2-Chip Hemocytometer and an optical microscope. Around 1x10^6 cells are added to 15 mL of media in a new T-75 flask, and then incubated at 37°C.

3.3 Cytotoxicity Determination

We determined the IC50 concentrations of choline octanoate, choline 2,2 dimethylhexanoate, choline 2-ethylhexanoate, and choline trans-2-octenoate.

In order to fully characterize this new batch of each IL, we determined the IC50 concentration with a cell counting kit-8 (CCK-8) assay. Murine 4T1 tumor cells were seeded at 10,000 cells/well and incubated to adhere overnight. Cells were treated to various IL concentrations 0% - 10% prepared via 1:3 serial dilution. The plate was incubated for 24 h. Upon incubation, supernatant was removed, and 10% CCK-8 solution was added. The plate was incubated again for one hour and absorbance was read on a spectrophotometer plate reader at 450 nm. IC50 was determined using GraphPad Prism analysis.

The IC50 concentrations of choline propanoate, choline hexanoate, choline heptanoate, and choline decanoate utilized in this study were previously determined in our lab.

3.4 Cell Death Mechanisms Investigation

Cell death mechanism assays were run on both the panel 1 (multi chain-length library) and panel 2 (choline octanoate isomer library). The protocol of each assay, as well as any differences in how the assay was run on each library, will be subsequently described.

3.4.1 Annexin V/Propidium Iodide (PI) Staining - Apoptosis Determination

This assay utilized the Invitrogen Molecular Probes FITC Annexin V/Dead Cell Apoptosis Kit with FITC annexin V and PI, for Flow Cytometry [83]. The assays were run according to the Invitrogen kit instructions. 4T1 cells were seeded at 100K cells/well in a 48-well plate and allowed to adhere overnight. ILs of both libraries were prepared at predetermined IC50 concentrations in complete media. Supernatants were removed and IL dilution or media only were added. After treatment, cells were incubated for 24 h. In order to harvest cells, supernatants were collected from plates, put into tubes, and centrifuged at 500 g for 5 minutes. Meanwhile, plates were treated with incubated trypsin at 37°C. After 5-10 minutes, the trypsin reaction was quenched with media. Cells pelted in centrifuged tubes were resuspended in trypsinized cells from the plate. Tubes were spun down again and washed with 200 µL of PBS. After harvesting, cells were stained with Annexin V and propidium iodide (PI) by being resuspended in an antibody stain. Controls were prepared using a mixture of live/dead cells. These cells were prepared by harvesting untreated cells, splitting them, and heat killing half of them by incubating at 60°C for 10 minutes. Then, live and dead cells were mixed and split into three wells, where they were treated with Annexin V, PI, or blocking buffer only. Cells were read by flow cytometry immediately after staining. Fluorescence emission was measured at 530 nm (FL1) and >575nm (FL3).

This assay was conducted separately on the straight-chain library (panel 1) and the choline octanoate isomer library (panel 2) using identical protocols.

3.4.2 Caspase-3/RIP3 Staining - Necroptosis/Apoptosis Determination

4T1 cells were seeded at 100K/well and incubated overnight for adhesion. Subsequently, negative control groups of cells were treated with 60 μM of necrostatin-1 incubated for 1 h. ILs of both libraries were prepared at predetermined IC50 concentrations in complete media. Cells were then treated with corresponding IL dilution with/without inhibitor or media only. Treated cells were incubated for 24 h. Next, cells were washed, harvested, fixed/permeabilized, then stained for caspase-3 and RIP3. Cells were read by flow cytometry.

This assay was conducted separately on the straight-chain library and the choline octanoate isomer library. There were a few differences in experimental conditions. First, within the straight-chain library, another control group of cells was included, treated with z-VAD-FMK (zVAD), an apoptotic inhibitor at 50μM. This step took place along with the necrostatin-1 pre-treatment of the negative control group. The isomer library was not treated with the zVAD control group to focus on assaying necroptosis only (not apoptosis). Second, the straight-chain library (panel 1) cell groups were treated in triplicate. The isomer library (panel 2) was treated in duplicate.

3.4.3 Lactate Dehydrogenase (LDH) Assay

Invitrogen™ CyQUANT™ LDH Cytotoxicity Assay Kit was used for this assay [84]. 4T1 cells were seeded at 5000 cells/well and were allowed to adhere overnight. Each IL in both the straight-chain library and the choline octanoate isomer library were diluted in complete media to IC50/2, IC50, IC50x2, and IC50x4 concentrations via a 1:2 serial dilution. Cells were treated with ILs of each concentration in triplicate. One triplicate group of No Treatment controls, as

well as two additional triplicate groups of cells were left to incubate for 24 h. The assay was then conducted according to the CyQUANT™ LDH Cytotoxicity Assay Kit Product Information Sheet. Control groups included spontaneous LDH and maximum LDH. After 24 h, Spontaneous LDH activity control was prepared by adding 10 µL of water to triplicate cell wells. Maximum LDH activity cells were prepared by adding 10 µL of lysis buffer to triplicate wells. Cells were transferred to a new plate, reaction mixture was added, then incubated 30 min at room temperature before adding 50 µL of stop solution. Absorbances were measured at 490 nm and 680 nm by a spectrophotometer plate reader. To determine LDH toxicity, the background value, measured at 680-nm absorbance, was subtracted from the 490-nm absorbance. In order to calculate cytotoxicity, the following formula was used.

$$\left[\frac{IL\ treated\ activity\ -Spontaneous\ LDH}{Maximum\ LDH-Spontaneous\ LDH}\right]*100=\%\ Cytotoxicity$$

Calculations and analysis were conducted via GraphPad Prism. This assay was conducted separately on the straight-chain library (panel 1) and the choline octanoate isomer library (panel 2) using identical protocols.

3.5 Immunogenicity Assays

During this study, immunogenicity assays were performed on the choline octanoate isomer panel (panel 2).

3.5.1 Calreticulin Exposure Determination

4T1 cells were seeded at 100 K cells/well in a 24 well plate and allowed to adhere overnight. Ionic liquids evaluated in the choline octanoate isomer panel were prepared at IC50 and IC50x2 concentrations via a 1:2 dilution in complete media. Supernatants were removed and IL dilution

or media only were added in triplicate. After treatment, cells were incubated for 24 h. Cells were harvested, and the supernatants were collected and frozen for future use in the ATP assay. Cells were washed prior to staining with calreticulin antibody. Cells were then stained with Live-Dead Blue (fixable stain) viability dye and incubated in the dark at 4°C. Then, cells were washed with a stain buffer and a binding buffer. Finally, the cells were treated with the antibodies and controls were prepared. Cells were fixed and stored at 4°C for 2-3 days. Calreticulin expression was determined with flow cytometry. Data were analyzed using GraphPad Prism. This experiment was run twice.

3.5.2 ATP Determination Assay

This assay utilized the Invitrogen ATP Determination Kit [85]. 4T1 cells were seeded at 100 K cells/well in a 24 well plate and allowed to adhere overnight. ILs evaluated in the choline octanoate isomer panel were prepared at IC50 and IC50x2 concentrations via a 1:2 dilution in complete media. Supernatants were removed and IL dilution or media only were added in triplicate. After treatment, cells were incubated for 24 h. Supernatants were collected and frozen to be stored in an -80°C freezer. Meanwhile, cells were harvested for calreticulin analysis. After 2-4 weeks frozen in storage, the supernatants were thawed in the dark. D-luciferin solution was prepared with reaction buffer, water, and D-luciferin. DTT stock solution was diluted. ATP standard curve solutions were prepared at various concentrations with a serial dilution. ATP standard reaction solution was prepared with Reaction Buffer, DTT, D-luciferin, and firefly luciferase. The standard solution treated all of the samples. Bioluminescence was measured on a plate reader. Standard curve results were then fitted to a quadratic model relating luminescence

and ATP concentration. ATP concentrations of luminescence averages of each sample were calculated using this model.

3.5.3 Autophagy Determination Assay

This assay was conducted with the CYTO-ID® Autophagy Detection Kit, according to the manufacturer's instructions [57]. This kit measures accumulated autophagic vesicles utilizing a 488 nm-excitable green dye. 4T1 cells were seeded at 50 K cells/well in a 24 well plate and allowed to adhere overnight. Ionic liquids evaluated in the choline octanoate isomer panel were prepared at IC50 concentration. One group of cells were pretreated with chloroquine, an autophagy inhibitor, at 50 μM concentration. After six hours, chloroquine treatment was removed, and cells were washed with PBS. Supernatants were removed from all non-chloroquine treated cells. IL dilution or media only were added in triplicate to both chloroquine-treated and non-chloroquine-treated cells. One group of triplicate wells were treated with rapamycin, an autophagy inducer. After treatment, cells were incubated for 16 h. Upon completion of the treatment period, cells were harvested in tubes and adherent cells were trypsinized. Cells were centrifuged at 1000 rpm for 5 minutes to pellet cells. Supernatants were collected and frozen in separate tubes for subsequent ATP release analysis. Cells were washed using cell culture media. 250 μL of diluted CYTO-ID Green stain solution was added to each sample. Samples were then incubated at room temperature in the dark for 30 minutes. Cells were then collected by centrifugation, washed with assay buffer, and resuspended in assay buffer. Cells were analyzed by flow cytometry in green (FL1) or orange (F2) fluorescence channels. This assay was only conducted on Panel 2: isomers of choline octanoate.

3.6 Data Analysis

Statistical analyses were conducted using GraphPad Prism. Significance and p values were determined using one-way ANOVA analysis and a post-hoc Tukey HSD. P-values ≤ 0.05 are denoted by a single star (*). P-values ≤ 0.01 are denoted by a double star (**)

4. Results

4.1 Ionic Liquid Synthesis

Ionic liquids were synthesized according to the chemical route shown in Figure 3. After the synthesis of choline trans-2-octenoate, the material appeared more translucent and crystallized rather than a viscous liquid, as the other materials (Figure 4). Thus, we attempted to remove water via extra rotary evaporation and vacuum oven incubation. However, the final material's physical appearance was still observed to be notably different than other ILs synthesized.

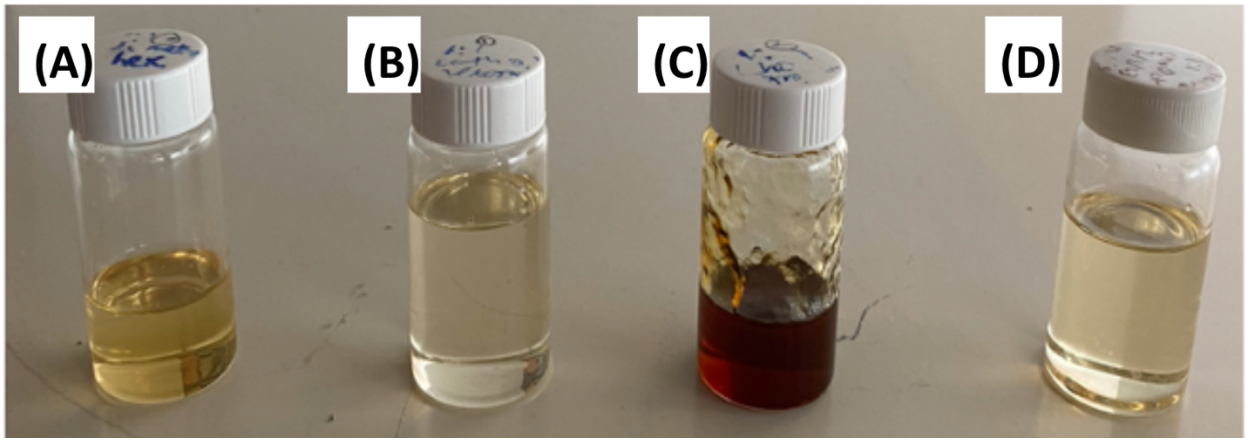

Figure 4. Ionic liquids synthesized. (A) choline 2,2-dimethylhexanoate (methyl-branched), (B) choline 2-ethylhexanoate (ethyl-branched), (C) choline trans-2-octenoate (unsaturated), and (D) choline octanoate (saturated/straight-chain). Each IL has eight carbons in its anion chain.

We analyzed the purity of the panel 2 ILs using nuclear magnetic resonance (NMR) spectroscopy (Figure 5). As shown in Table 1, all ILs were synthesized at a near 1:1 choline:acid ratio.

Table 1. Choline : Acid Ratio reported by NMR Spectroscopy

Compound	Choline : Acid Ratio
Choline 2,2-dimethylhexanoate (methyl-branched)	1.36
Choline 2-ethylhexanoate (ethyl-branched)	1.11
Choline trans-2-octenoate (unsaturated)	1.20
Choline octanoate (saturated/straight-chained)	0.84

However, NMR spectra showed an extra, anomalous peak from the choline trans-2-octenoate sample (Figure 5C). This suggests that this ionic liquid was not fully and completely formed properly, which aligns with our observations of its translucent, crystalline appearance.

4.2 Cytotoxicity

IC50 concentrations of each IL were determined by the CCK-8 colorimetric viability assay. The IC50 values, in vol/vol % demonstrate that ionic liquids of increasing carbon chain length exhibit more cytotoxicity (Table 2) and that increasing branched character exhibits less cytotoxicity compared to straight-chain octanoate (Table 3). Moreover, choline trans-2-octenoate, with its unsaturated double bond, also is less cytotoxic than choline octanoate.

These results support the hypothesis that the ILs with less lipophilic anions are less cytotoxic (Figure 6). It appears that adding a double bond in the IL anion leads to a less pronounced decrease in cytotoxic activity than the decrease resulting from adding branching to the IL anion. Between the two branched anions, the ethyl-branched was more cytotoxic than the methyl branched (Table 3). This decrease in cytotoxicity aligns with the general trend of decreasing lipophilicity (Table 4) [64], [100]. Table 4 shows lipophilicity reported in the literature for the acids used in each IL panel. Lipophilicity increases with carbon chain length and decreases with addition of branching or double bond (for acids of constant carbon chain length). Lipophilicity is reported as the partition coefficient of the acid with water (log P).

Table 2. IL Panel 1: IC50 values of ILs with various anion carbon chain lengths on 4T1 cells - *Except for Choline Octanoate, these values were previously determined by Danika Rodrigues.*

Compound	IC50 Value (vol/vol %)
Choline hexanoate	0.745
Choline heptanoate	0.319
Choline octanoate	0.098
Choline decanoate	0.084

Table 3. IL Panel 2: Determined IC50 values of ILs with various structures of eight-carbon anion chains

Compound	**IC50 Value (vol/vol %)**
Choline 2,2-dimethylhexanoate	0.400
Choline 2-ethylhexanoate	0.266
Choline trans-2-octenoate	0.124
Choline octanoate	0.098

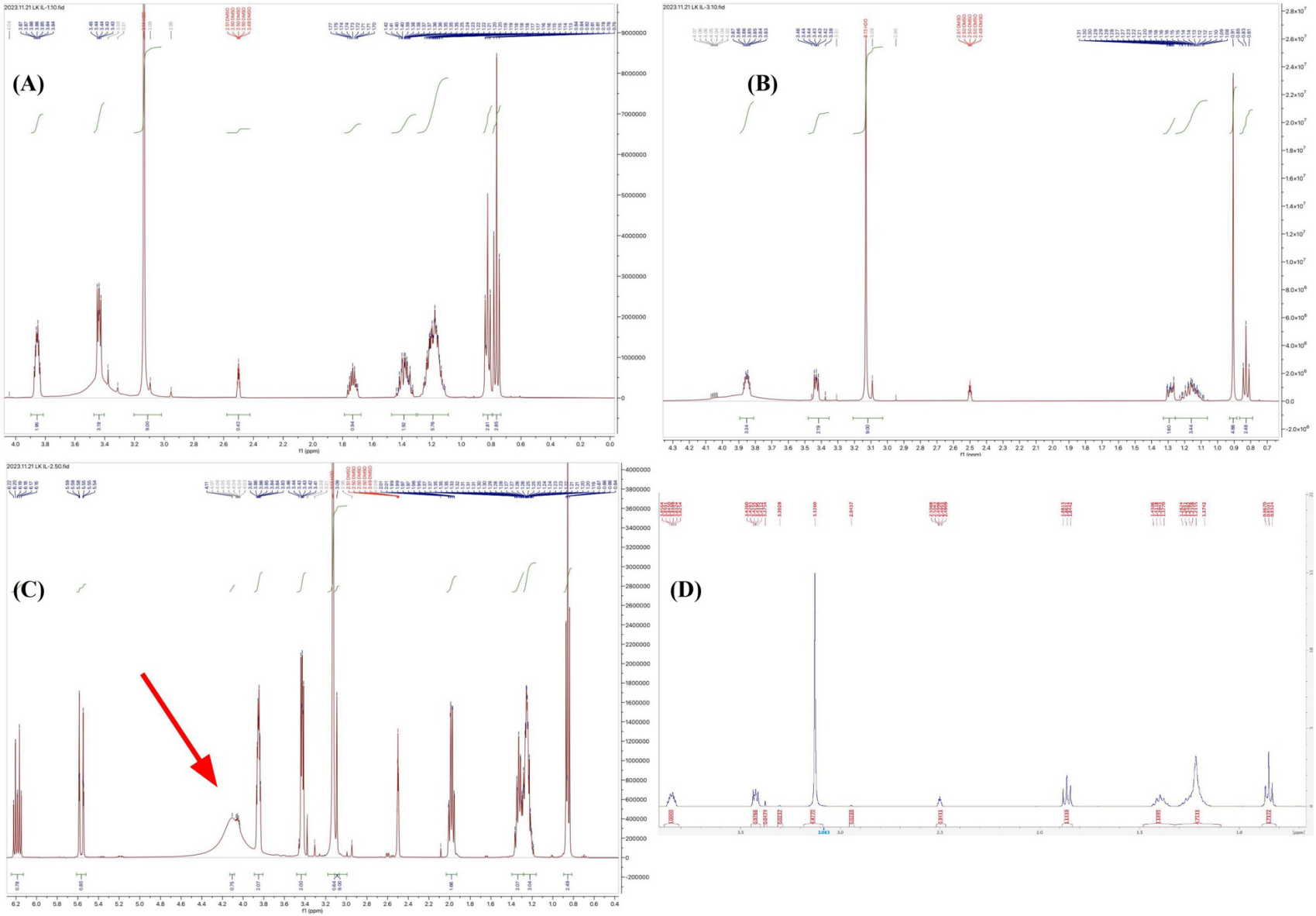

Figure 5. NMR spectra of (A) choline 2,2-dimethylhexanoate, (B) choline 2-ethylhexanoate, (C) choline trans-2-octenoate, with aberrant extra peak highlighted with red arrow, and (D), choline octanoate. Results were collected in collaboration with Danika Rodrigues.

Table 4. Lipophilicity of ILs in Panel 1 and Panel 2 reported in literature.

Source: PubChem - NIH

Compound	Log(P) value	Literature Reference(s)
Panel 1		
Hexanoic Acid	1.9 – 1.92	[86], [87]
Heptanoic Acid	2.42 – 2.5	[88], [89]
Octanoic Acid	3 - 3.05	[81], [90]
Decanoic Acid	4.09 – 4.1	[91], [92]
Panel 2		
2,2-Dimethylhexanoic Acid	2.6	[80]
2-Ethylhexanoic Acid	2.6	[82]
Trans-2-octenoic Acid	2.7 – 2.9	[79], [93]
Octanoic Acid (same as above)	3 - 3.05	[81], [90]

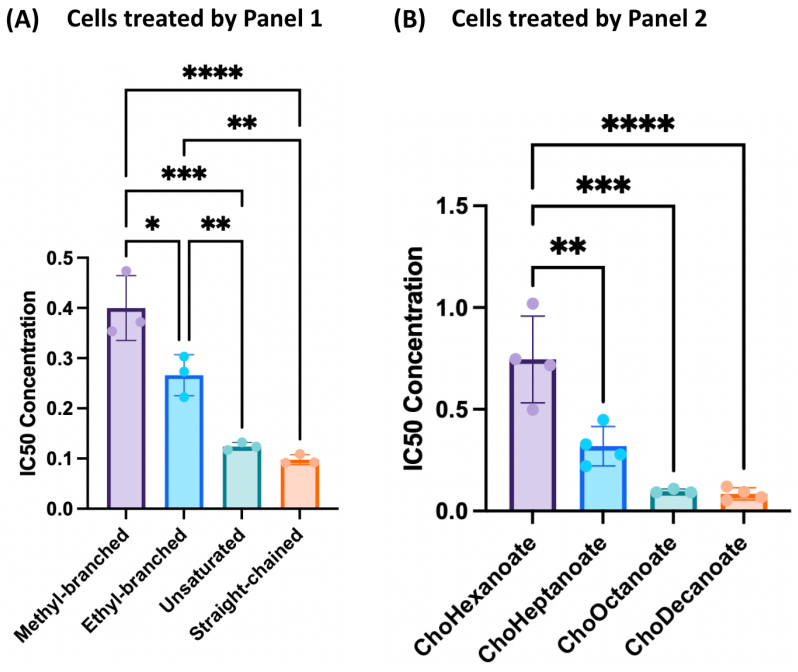

Figure 6. IC50 concentrations of (A) cells treated by Panel 1, choline-based ILs with anion chains of increasing anion carbon chain length (*data previously collected by Danika Rodrigues*) and (B) cells treated by Panel 2, choline-based ILs whose anions are isomers of octanoate (n=3).

4.3 Cell Death Mechanisms

4.3.1 Annexin V/Propidium Iodide (PI) Staining - Apoptosis Determination Results

The Annexin V/PI stain was run on cells treated with IL Panel 1 and Panel 2. First, in order to understand the degree to which apoptosis is implicated in cell death induced by ILs whose anions have varying carbon chain lengths, we ran this assay on Panel 1. We compared cells treated with each IL at both IC50 and IC50x2 concentrations as well as no treatment control cells. Live cells are identified as annexin V-/PI-. Evidence of early apoptosis is indicated by annexin V+/PI- results, and late apoptosis is indicated by annexin V+/PI+ results (Note: we do not consider annexin V+/PI+ to indicate necrosis, as corroborated in section 4.3.2). Additionally, necrotic cells are indicated as Annexin V-/PI+ [94].

Compared to untreated cells, 4T1 treated with ILs across Panel 1 show a trend that as concentration is doubled, cells shift from majority live cells (annexin V-/PI-) in the No Treatment group to early apoptotic (annexin V+/PI-) and to late apoptotic (annexin V+/PI+) states (Figure 7). This trend is observed in every IL. However, there is a less complete shift for cells treated by choline hexanoate and choline octanoate. Across all treatment groups, necrotic activity (annexin V-/PI+) was largely not observed, as evidenced by low percentages of annexin V-/PI+ cells.

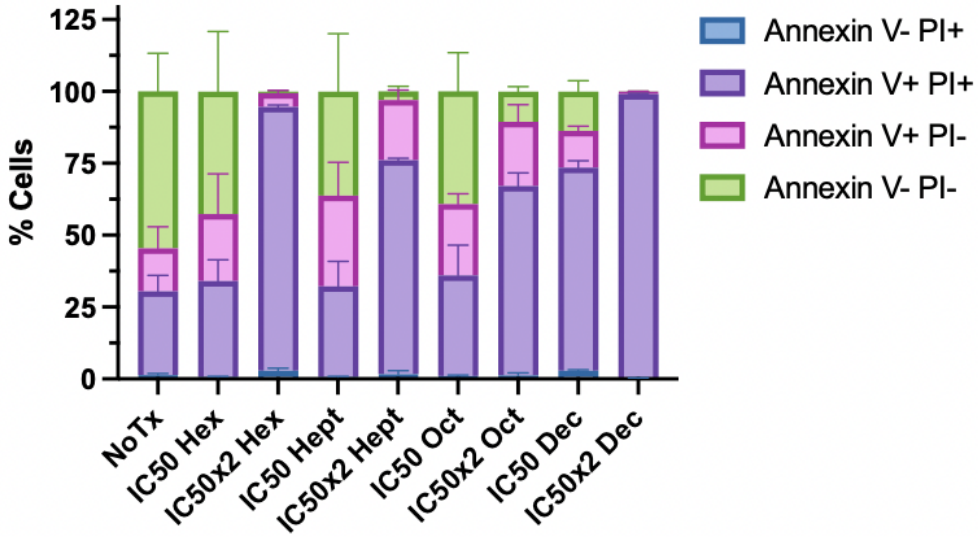

Figure 7. Cells demonstrating Annexin V and PI binding when treated with each IL in Panel 1 (anions with increasing carbon chain lengths) at IC50 and IC50x2 concentrations (n = 3). Percentage of cells read out in each quadrant, indicating phase of death.

The assay was repeated for cells treated by IL Panel 2. No Treatment control group results were excluded because various experimental conditions caused their death rates to appear than those in the IL treatment groups (the reasons for this are discussed in the Discussion

section). Here, 4T1 cells treated at higher IL concentrations (with the exception of the ethyl-branched IL) (Figure 8B) trend similar and slightly increased evidence of early apoptosis (annexin V+/PI-) and late apoptosis (annexin V+/PI+) with those treated at lower IL concentrations (Figure 8A). Again, low levels of annexin V-/PI+ cells indicate low necrotic activity. However, cells treated with the ethyl-branched IL demonstrated a marked decrease in both early and late apoptotic activity with a doubling of IL concentration. Generally, cells treated with the straight-chain choline-octanoate have higher rates of early and late apoptotic activity compared to cells treated with the branched or unsaturated ILs (Figure 8). This suggests that apoptotic activity can be selected for by treating with the straight-chained choline octanoate compared with its other eight-carbon anion isomers.

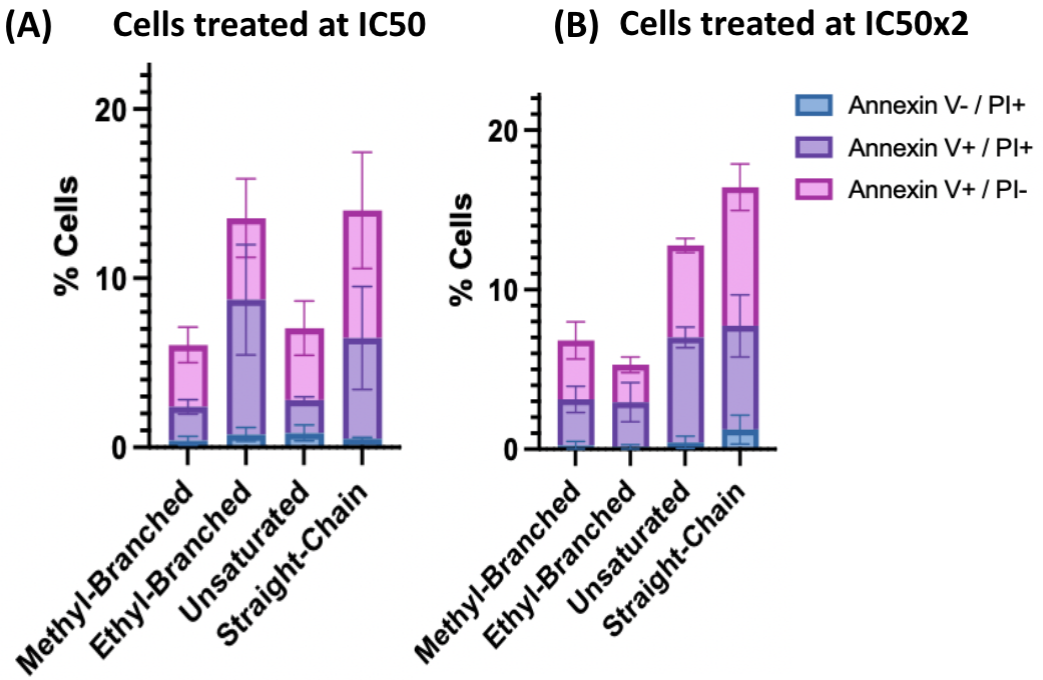

Figure 8. Cells demonstrating Annexin V and PI binding when treated with each IL in Panel 2 (anions with increasing carbon chain lengths) at IC50 and IC50x2 concentrations (n =

3). Percentage of cells read out in each quadrant, indicating phase of death. Live cells (Annexin V-/PI-) were omitted from the figure for clarity of results.

4.3.2 Lactate Dehydrogenase (LDH) Assay - Necrosis Determination Results

The LDH determination assay was run on cells treated by ILs in Panel 1 and Panel 2. In Panel 1, the LDH levels trended similarly between all groups (Figure 9A). In Panel 2, LDH levels for choline octanoate exceeded that of its isomers at IC50x4 and LDH levels for its ethyl-branched isomer was notably less than the other groups (Figure 9B). However, in all groups of cells treated in each panel, LDH levels did not approach the positive control. This suggests relatively low levels of necrotic cell death induced by all ILs tested. These data corroborate the results of the annexin V/PI assay, which also did not show evidence of necrosis as the primary death pathway. They also support our understanding that the increased percentage of cells exhibiting Annexin V+/PI+ staining at IC50x2 compared to at IC50 is evidence of late apoptosis rather than of necrosis [48].

The positive control shown in Panel 2 (Figure 9B) was calculated during Panel 1 experiment (Figure 9A), because during Panel 2, the calculated positive control appeared artificially high, due to experimental conditions during assay processing.

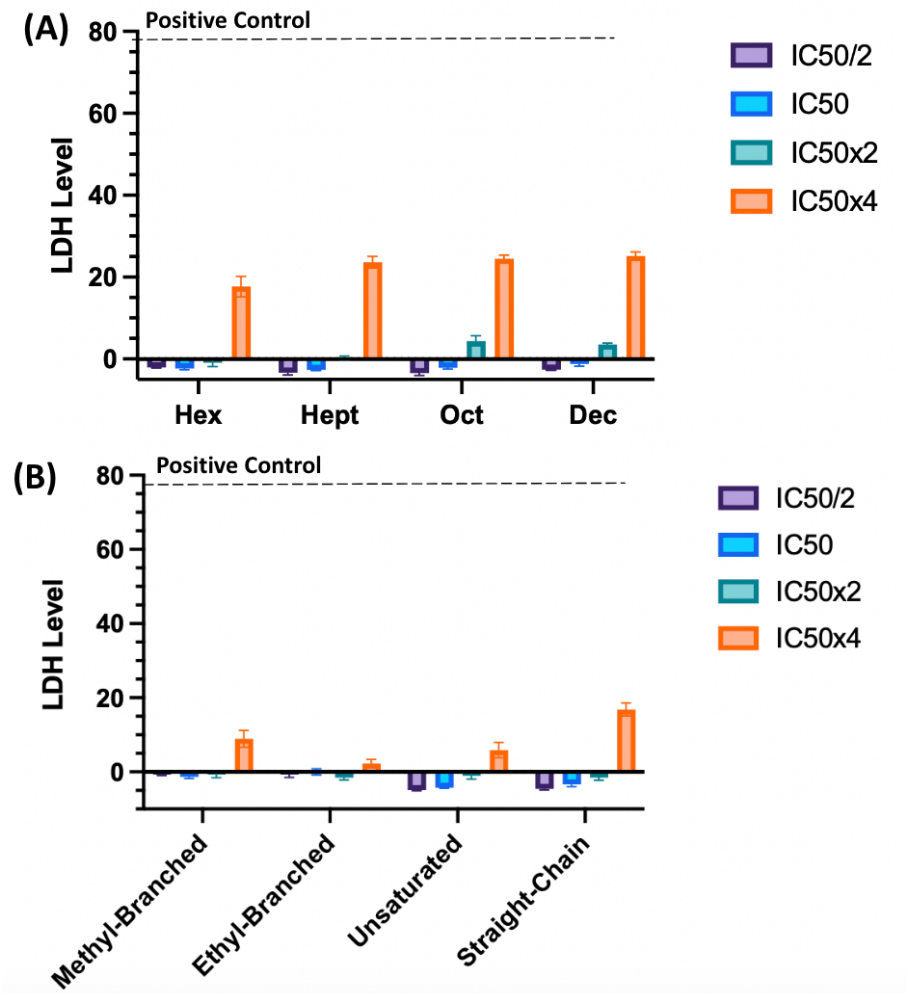

Figure 9. LDH assay readout of 4T1 cells treated with a panel of ILs with increasing anion carbon chain lengths (n=3) (B) panel of isomers to choline octanoate (n=4). Both panels were treated at increasing concentrations ranging from their respective IC50/2 to IC50x4 values.

4.3.3 Necroptosis/Apoptosis Determination - RIP3/Caspase-3 Staining

We conducted necroptosis determination assays via staining for RIP3/Caspase-3 (Casp-3) in cells treated by each panel. First, we examined cells treated by Panel 1. When apoptosis is inhibited via treatment with zVAD, choline octanoate-treated cells show a significant decrease in Casp-3 expression, compared to when it is not inhibited (Figure 10A). This suggests apoptosis as

a cell death pathway for choline octanoate. However, when necroptosis is inhibited with necrostatin-1, there is not a statistically decrease in RIP3 expression for any IL treatment (Figure 10B). This suggests that necroptosis is not the primary pathway induced by the IL panel.

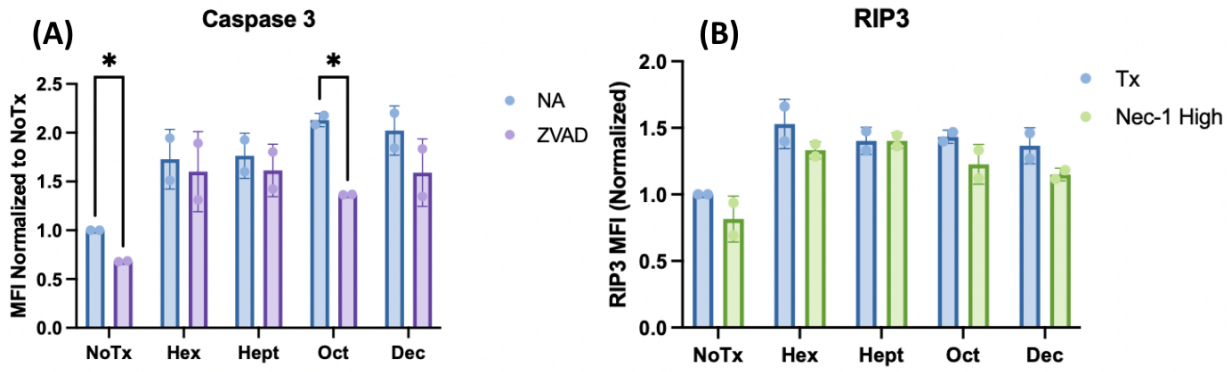

Figure 10. Expression of (A) Caspase-3 compared to apoptosis inhibitor control (zVAD) and (B) RIP3 compared to necroptosis inhibitor control (Nec-1) by cells treated by IL Panel 1 at [IC50x2] (n=3). Expression is represented by normalized Mean Fluorescence Intensity (MFI). In collaboration with Danika Rodrigues.

Cells were then treated by Panel 2. Here, they were not subject to a zVAD control to home in on necroptosis instead of apoptosis. In this study, Casp-3 and RIP3 treated cells were subject to a necroptosis inhibitor control (Nec-1). IL-treated cells appeared to demonstrate a higher expression of Caspase-3 compared to No Treatment groups (Figure 11A). This corroborates the relevance of apoptosis in cell death with the previous cell death pathway assays, as Caspe-3 is widely expressed in apoptotic cells [95]. However, across all groups, RIP3 expression does not appear to significantly decrease with Nec-1 treatment (Figure 11B). This suggests that

necroptosis may not be a primary IL-induced cell death pathway for these ILs tested.

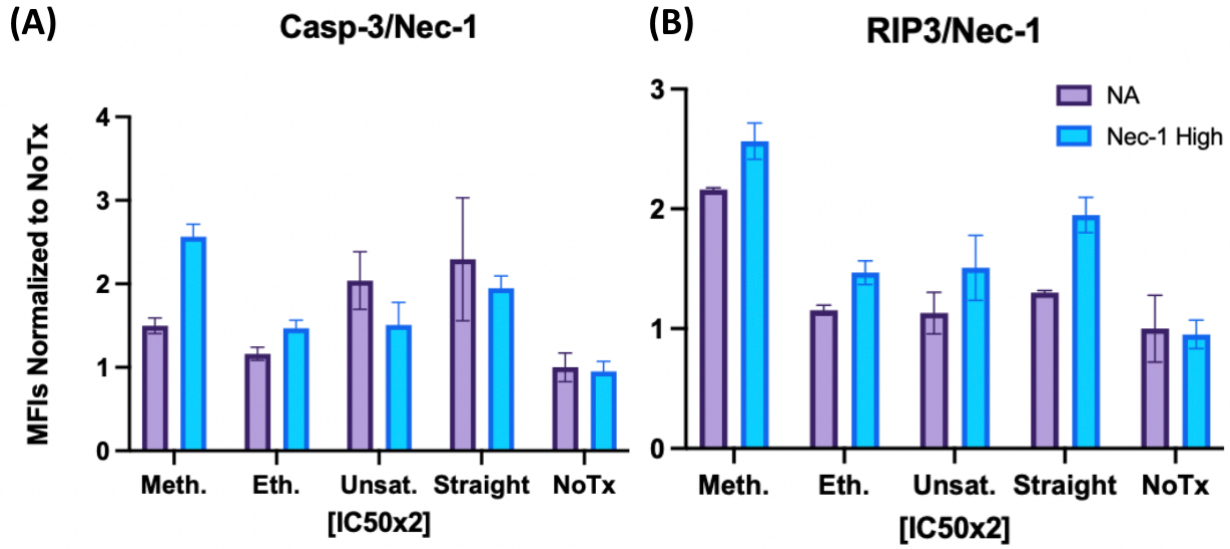

Figure 11. Expression of (A) Caspase-3 and (B) RIP3 by cells treated by IL Panel 2 at [IC50x2] compared to necroptosis inhibitor control (Nec-1) (n=2). Expression is represented by normalized Mean Fluorescence Intensity (MFI). In collaboration with Danika Rodrigues.

4.4 Immunogenicity

Immunogenicity markers were assayed on cells treated by Panel 2 only.

4.4.1 ATP Determination

We ATP release of cells treated with the IL panel of choline octanoate isomers at [IC50] and [IC50x2]. Due to the noisy results of this sensitive luminescence-based assay, we took the mean of luminescence readouts before applying a quadratic model to approximate ATP concentration. The model was calculating using quadratic regression of standard curve controls.

Trends indicate an ATP concentration increase in the supernatants of cells treated with increased concentration of ILs (Figure 12). The results of this assay suggest that at [IC50x2], there is an IL-induced release of ATP compared to no treatment cell groups.

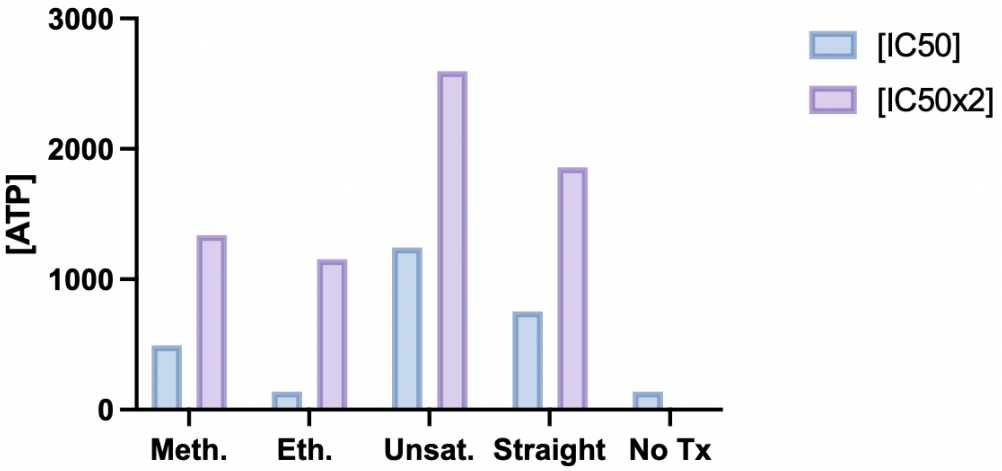

Figure 12. ATP concentration (nM) in the supernatants of cells treated with each Panel 2 IL at [IC50] and at [IC50x2] as well as the no treatment group. During the analysis of this assay's results, the mean of luminescence readings (n=3) was taken before applying the concentration model to the average (n=1) in order to reduce noise of the assay.

4.4.2 Calreticulin Staining

We assayed 4T1 cells treated by IL panel 2, the isomers of choline octanoate. Here, for the unsaturated IL, doubling the IC50 concentration leads to a significant increase in calreticulin expression. Doubling concentration appears to result in a trend of increasing CRT in the methyl-branched IL and in straight-chain choline octanoate as well. Additionally, choline octanoate at IC50x2 induced significantly more CRT expression than the methyl-branched IL at IC50, the ethyl-branched IL at both IC50 and IC50x2, and the unsaturated IL at IC50 (Figure 13). This suggests that the presence of branching in the IL anion may correlate with reduced

immunogenicity of cell death compared to anion without branching. Moreover, at [IC50] the presence of a double bond in the IL anion may also correlate with reduced immunogenicity of cell death compared to anions without unsaturation, though this was not observed at IC50x2.

The expression of CRT in the No Treatment group was notably higher than any other group, potentially influenced by experimental set up considerations, which will be elaborated upon further in the Discussion section.

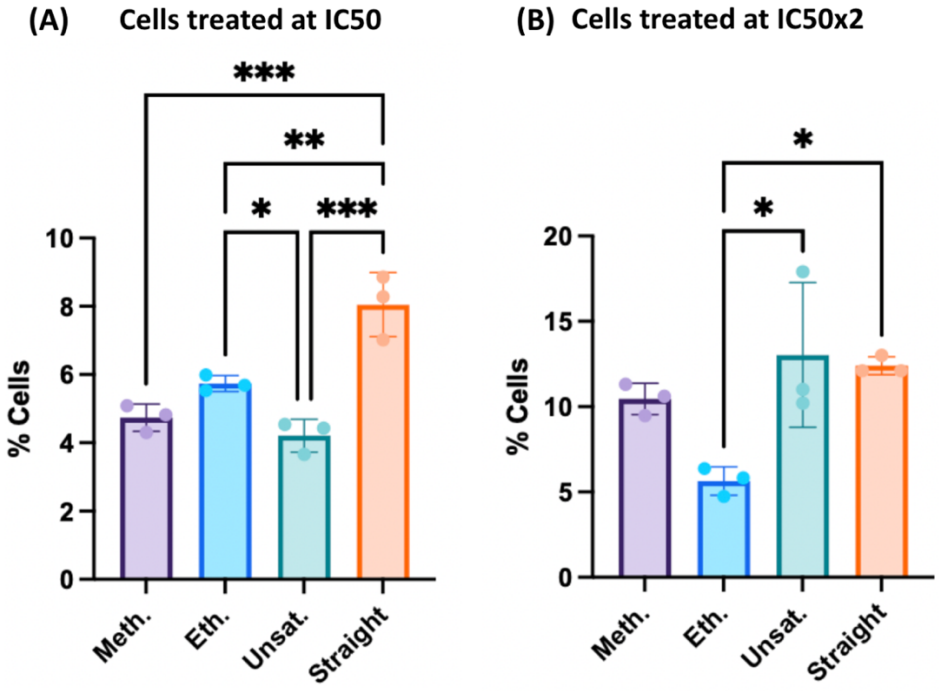

Figure 13. Calreticulin exposure in cells treated by Panel 2 ILs at (A) IC50 and (B) IC50x2 (n=3).

4.4.3 Autophagy Determination Assay

Autophagy induction was assayed on cells treated by IL Panel 2 only. Autophagy was not found to be significantly implicated in IL-induced cell death. As expected, most of the chloroquine

treated groups, which were negative-control autophagy inhibitors, demonstrated significantly less autophagy signal than the rapamycin treated group, which was a positive-control autophagy inducer. Compared to the rapamycin positive control, there was a significantly lower autophagy signal in both IL-only for choline 2,2-dimethylhexanoate and in the choline 2-ethylhexanoate IL treatment (Figure 14A). Although the unsaturated and straight chain ILs did not have a statistically significant difference compared to the rapamycin control, the trend of lower signal was consistent. Moreover, there was no significant difference—nor consistent trend—between IL-only treatment groups directly with their respective chloroquine-IL treatments (Figure 14B). This further corroborates the suggested lack of autophagy induced by IL treatment.

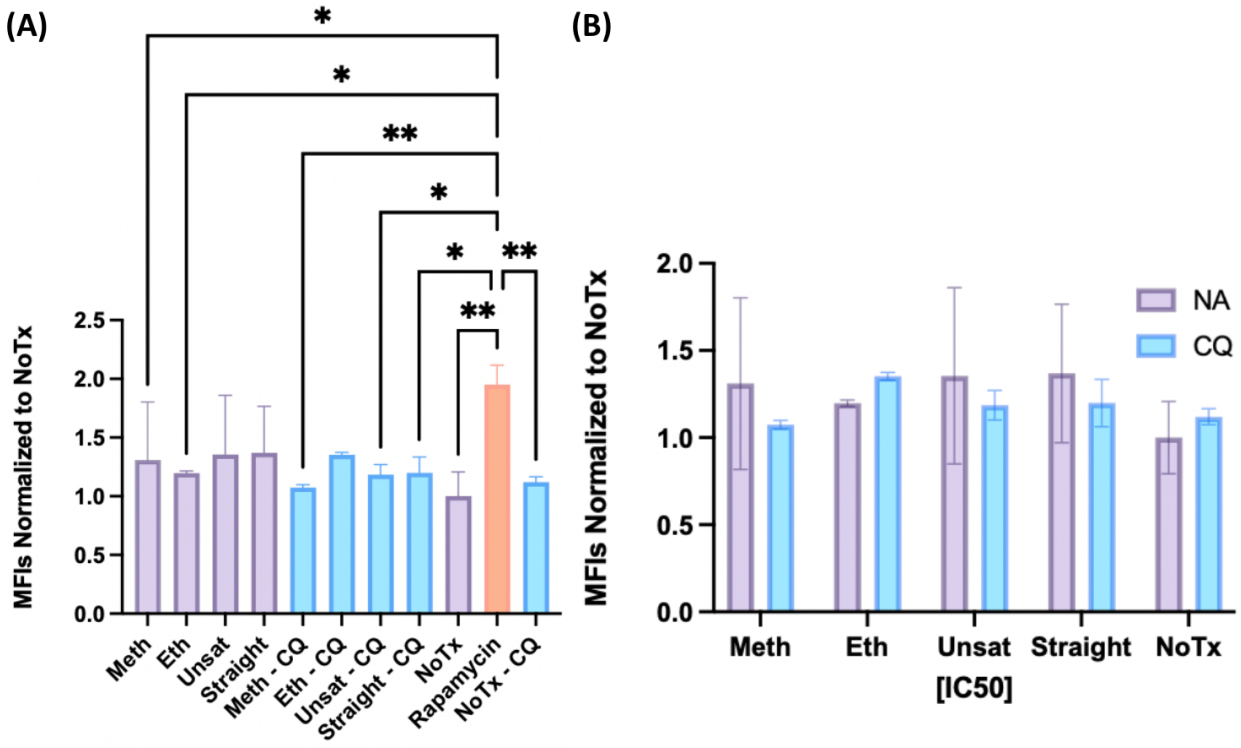

Figure 14. Autophagy-related signal displayed as Mean Fluorescence Intensity (MFI) normalized to the No Treatment group of (A) each Panel 2 IL displayed with their respective chloroquine-treated negative control as well as a rapamycin treated positive control. (B) Direct side-by-side comparison of each IL with their respective chloroquine-treated negative control

(n=3). All IL-treated cells were treated at the IL's IC50 concentration. Chloroquine treated groups were pre-treated at 50 μM, and the Rapamycin control group was treated at 10 μM.

An ATP release detection assay on the supernatants of these cells further supported the release of ATP in IL-induced cell death (Figure 15). It is worth noting that the trend of ATP release for the choline 2-ethylhexanoate IL is different between the present study and the ATP release assay conducted in 4.4.1. This may be an artifact of the sensitivity of luminescence-based assays, which we attempted to mitigate by averaging luminescence signals before applying the ATP concentration model, as shown in Figure 15.

When autophagy is inhibited by the chloroquine treatment, there is a very notable decrease in ATP release. Moreover, the rapamycin-treated group, in which autophagy was induced, there was not an observed comparatively strong signal for ATP release compared to IL-treated groups.

While the autophagy staining did not reveal major trends in IL-only versus IL + Chloroquine treatment, the ATP release difference between the two types of treatments may suggest that nuances in the role that autophagy plays in ATP release, because although autophagy was not shown to be implicated (Figure 14), ATP release appeared to be suppressed by the autophagy inhibitor (Figure 15). This is further discussed in the *Discussion* section.

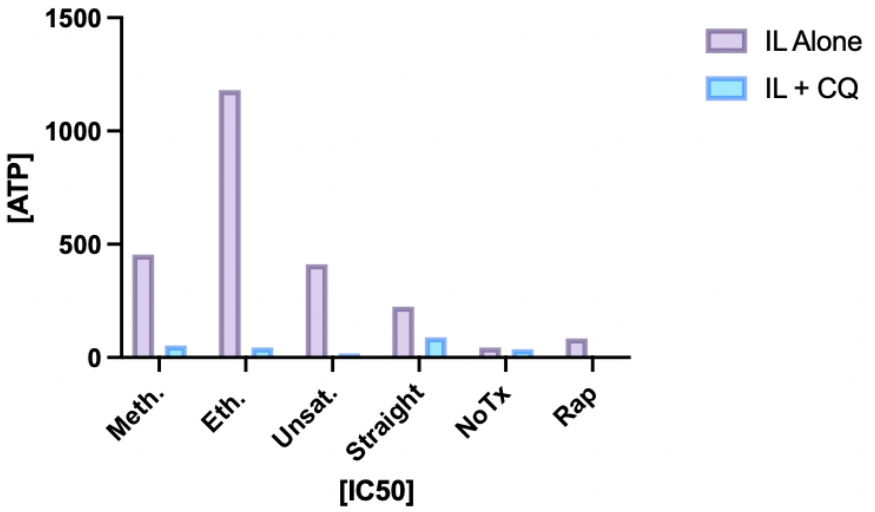

Figure 15. ATP concentration in (nM) of supernatants from cells treated with each Panel 2 IL either alone or along with chloroquine, an autophagy inhibitor. ATP levels of treatment controls, and cells treated by rapamycin, an autophagy inducer, were also included. During the analysis of this assay's results, the average of luminescence readings (n=3) was taken before applying the concentration model to the average (n=1) in order to reduce noise of the assay.

5. Discussion

5.1 IL Synthesis

Synthesis of ILs with saturated anions was successful, but the synthesis of choline trans-2-octenoate proved more challenging. An anomalous peak appeared in its NMR readout, suggesting that this IL was not fully and completely formed properly. Despite it appearing crystalized, it was still functionally in liquid form, and we were able to successfully and accurately pipette desired volumes during our investigations. The exact cause of this IL's inability to form well has not been determined. It is still unclear how the crystalized, somewhat anomalous formation of this IL affected its readouts. In order to understand the effect of the

formation impurity, future investigations may attempt to reform this IL using optimized synthesis conditions, such as slower dropwise addition of components or longer heating period in the oven. Moreover, it would be useful to understand how other unsaturated ILs compare to choline trans-2-octenoate, both in physical properties and interacting with cells.

5.2 Cytotoxicity

Previous work from our lab (collaboration with Danika Rodrigues) determined the IC50 concentrations of ILs in Panel 1 and found that the cytotoxicity of ILs increases with length of carbon anion chains, corresponding to increasing lipophilicity. During this study, our cytotoxicity screens demonstrated that of the ILs that we surveyed in Panel 2, choline octanoate was the most cytotoxic. This aligns with our initial hypothesis that ILs with anions of the same number of carbons, eight, those with more carbon branching exhibit less cytotoxicity compared to unbranched octanoate. Notably, this appears to be a highly tunable phenomenon, as the methyl-branched IL appears to be much less than the ethyl-branched IL. Moreover, the unsaturated-anion IL also is less cytotoxic than choline octanoate, supporting the hypothesis that unsaturation decreases cytotoxic activity. Again, we hypothesize that decreased lipophilic activity caused by branching or unsaturation is the cause of the decreased cytotoxic activity due to the reduced hydrophobic interactions of the ILs with the cell membrane [71], [96]. Cytotoxicity is easily tunable, and future applications of ILs in whole tumor vaccines and beyond may be able to be optimized by modulating carbon chain length, branching, or double bonds in IL anions.

Another observed phenomenon is the similarly high cytotoxicity of the straight-chained choline octanoate and its unsaturated isomer compared with the much lower cytotoxicity of the methyl-branched and ethyl-branched isomers. Both the methyl- and ethyl-branched ILs have six carbons in their main chain, with two additional carbons branched. These two ILs have very similar lipophilic properties, as reported by their partition coefficient (Table 4). Thus, it is possible that these two ILs act similarly to choline hexanoate, which has been determined to have much lower cytotoxic activity than choline octanoate. It follows then that the unsaturated IL, which has eight carbons in its main anion carbon chain, may behave more similarly to straight-chained choline octanoate than the ILs with branched anions. However, it is worth noting that the lipophilicity/patrician coefficient of the branched acids, 2.6, is closer to that of octanoic acid (3-3.05, compared to that of hexanoic acid, 1.92 (Table 4).

5.3 Immunogenicity

Our ATP study showed a concentration dependent increase of ATP release for all ILs. ATP is an important marker of immunogenic cell death, so this is a notable corroboration of IL-induced ICD [97]. This will be further examined in the *Autophagy* section. Because of the study's noisy data release, we are unable to comment on the tunability of ATP release induced by ILs of different structures, though more iterations of this experiment on a more frequent time courses may better elucidate any anion structure-dependent change in ATP release. In future experiments, we will also re-examine ATP release by using greater populations of IL-treated 4T1 cells and by using either colorimetric or fluorescence-based assays.

Moreover, the CRT screen demonstrated that compared to straight-chained choline octanoate, ILs with branched anions (i.e. choline 2,2-dimethylhexanoate and choline 2-ethylhexanoate) may express lower levels of CRT, and ILs with double bond in the anion (trans-2-octenoate) also may express lower levels of CRT. This supports the original hypothesis that presence of carbon branching or double bond in the ionic liquid anion results in less immunogenicity of cell death. Again, this may be explained by lipophilicity, as more lipophilic compounds interrupt lipid homeostasis and may interfere with endoplasmic reticulum (ER) function [98]. CRT is an immunogenic marker released when the ER is stressed, so we infer that adding a double bond or branching into an ionic lipid anion reduces the lipophilicity, ER stress, and CRT expression of 4T1 cells.

The expression of CRT was higher in the No Treatment cell groups than in any other groups., which we attribute to a shortcoming in the experimental design We believe this is because during the treating and harvesting procedure, cells treated underwent substantial processing that resulted in lower cell counts. Moreover, for all cell groups, we tried to reach confluence before treatment. This likely led to over-confluence in cells in No Treatment group, which in turn meant that there was not enough space or media nutrients for the culture to remain healthy. As a result, these groups underwent cell death processes. In future experiments, this can be mitigated by using freshly prepared, health no treatment controls cultured in separate plate or flask than the experimental groups.

In future experiments, we will also evaluate the expression of other immunogenic markers, such as high-mobility group box 1 (HMGB1), Type I Interferon (IFN), and interleukin 1-β (IL-1β) [8].

5.4 Cell Death Pathways

Our results support the potential tunability of the magnitude of apoptotic activity based on IL treatment. The apoptosis assays conducted on both Panel 1 and Panel 2 suggested that cells were experiencing a shift from live cells to apoptotic cells (both early and late). During the apoptosis investigation of cells treated with Panel 1 ILs, there appeared a clear shift from a high percentage of live cells in the No Treatment group to early apoptotic cells in cells treated at [IC50] of each IL to late apoptosis in cells treated at [IC50x2]. As previously noted, there is a less complete shift towards apoptotic activity for cells treated by choline hexanoate and choline octanoate compared to cells treated by other IL anion carbon chain lengths (Figure 7). While the cause of this is unknown, it is useful context for the results of the Annexin V/PI assay on cells treated with IL Panel 2 (Figure 8). In this assay, there was a high percentage of live cells and a less clear shift between early and late apoptotic between [IC50] and [IC50x2] cells. Interestingly, there seemed to be a higher percentage of apoptotic cells when treated at [IC50] compared to [IC50x2] by the ethyl-branch IL.

The variation in stage of apoptosis induced by ILs is notable. Previous literature suggests that early apoptosis and apoptotic inactivation is the most preferable stage for cancer vaccines [99], [100], [101], while other studies have noted potential immunogenic benefits in late apoptosis [102], [103], [104]. The ability for different IL structures to hone on different apoptotic stages

may be significant for future studies that probe on the utility of these stages for ICD across cancer types.

During this panel, No Treatment cells appeared to have higher rates of death than the other groups. Like in the calreticulin study, this was very likely due to the over confluence of cells during when the cells were read. In future experiments, this can be mitigated by using freshly prepared, health no treatment controls cultured in separate plate or flask than the experimental groups.

During our investigation of necrosis as a potential cell death pathway, LDH results suggested that the ILs in our panel did not induce necrosis as the primary mechanism of cell death in 4T1 cells. A strong signal was only observed when cells were treated by ILs at [IC50x4], and even then, they did not approach the positive control. The higher necrotic activity at [IC50x4], which is a much higher concentration than we have used in any assay, is not surprising because ionic dysregulation prompted by high IL concentration can lead to swelling and necrosis [105], [106]. The low necrotic activity at IC50/2, IC50, and IC50x2 is notable because necrosis is often associated with toxin exposure, and previous work in the literature demonstrates that imidazolium-based ILs induce necrosis-dependent cell death related to cell membrane damage [107]. However, our choline-based ILs are able to induce ICD at [IC50] and [IC50x2] without inducing necrosis. As previously noted, this supports the conclusion that during the apoptosis study, cells that stained Annexin V+/PI+ were late-apoptotic cells, not necrotic cells. This is also significant because previous work has found that whereas apoptotic whole tumor cell vaccines produce an immune response in four different *in vivo* tumor models, necrotic cells do not [108].

The relevance of apoptosis was corroborated by subsequent assays, particularly the RIP3/Caspase-3 staining, in which IL-treated cells increased in Caspase-3 expression compared to no treatment cells. This was present in cells treated by Panel 1 (Figure 10A) and by Panel 2 (Figure 11A). These results are notable because of the caspase-3 can be involved in inducing immunogenic apoptosis [12]. The RIP3/Caspase-3 staining also suggested that necroptosis is not significantly implicated in IL-induced cell death because RIP3 expression, a necroptotic marker, was not reduced by the inhibition of necroptosis through nec-1. This trend was again observed in both Panel 1 (Figure 10A) and Panel 2 (Figure 10B). Thus, we can deduce that observed characteristics of regulated cell death appear to support apoptosis and not necroptosis.

Our study therefore demonstrates the tunability of magnitude and stage of apoptosis, as well as IL-induced cell death broadly between various types of ILs, even though tuning between various cell death pathways by modulating the chemical structure of the anion was not determined within our choline-based IL panels.

5.5 Autophagy

The autophagy determination assay did not reveal a significant change in autophagy between each IL treatment and the IL + chloroquine treatment, which inhibits autophagy. However, there was a significant increase in autophagy signal in the positive control rapamycin group, which confirmed the sensitivity of the assay. Interestingly, ATP release *was* observed to notably increase in IL treatment groups compared to the IL + chloroquine treatment groups. Although

rapamycin treatment appeared to result in a slightly higher ATP concentration than the No Treatment groups, it was notably lower than any of the IL treated groups.

Chloroquine is well-documented as reducing ATP [41], which is expected since it is an autophagy inhibitor, and autophagy induces ATP release [60], [109]. Rapamycin has been found to preserve ATP levels and it has been shown to increase ATP availability. However, in other studies, it also has been shown to maintain steady-state ATP concentration rather than increase it [110], which appears to align with the results of our experiment (Figure 15). Given these previously reported activity of our controls, we can suggest that our Panel 2 ILs may not have induced autophagy sustained until 24 hours and may have induced ATP released via another pathway [111].

Interestingly, previous work in our lab has shown that treatment with certain ILs can lead to a significant decrease in ATP. Albadawi et al. used an IL formulation (CAGE) that included a 1:1 choline to geranic acid ratio to treat cancer cells, both alone and in combination with doxorubicin [69]. Geranic acid includes 10 carbons with two methyl-branched substituents at the 3 and 7 carbons as well as a double bonds [112]. This study noted that the decrease in ATP as a result of CAGE treatment was important because cancer cells can resist treatment by switching to glycolysis to continue producing ATP, and that the IL may have prevented this form of resistance [69]. It is worth noting, however, that glycolysis is closely and inversely linked with autophagy and that in other work, the inhibition of autophagy has also been in targeted in combination with inhibiting glycolysis [61]. In fact, inhibition of autophagy, by agents including chloroquine, have been used to sensitize tumor cells to chemotherapy [113] [114]. Thus, while

autophagy and its subsequent ATP release can be involved in immunogenic cell death, autophagy can *also* be implicated in other, tumor-promoting pathways. Therefore, the lack of a strong autophagy signal (while detecting potentially ICD-induced ATP release) detected by our experiment may not be reflective of insufficient immunogenic cell death but rather of other IL-induced effects that could be useful for inhibiting tumor growth.

There are a couple of potential explanations for the results that we observed. One is that our ILs induced ICD, and that ATP release was facilitated by autophagy-independent pathways, such as by pannexin 1 ion channel mediation [111], [115]. Alternatively, IL inducement and subsequent inhibition of autophagy (or vice versa) could have occured over time [116]. In our experiment, cells were treated with Panel 2 ILs for 24 hours before their supernatants were collected for subsequent ATP determination assays. Albadawi et al. treated cells with CAGE on a time course and saw a significant decrease in ATP from 10h to almost no ATP at 24h [69]. In future experiments, a time course will be introduced to probe for any autophagy inducement or suppression over time, along with furthering our understanding of ATP release (Figure 12 and Figure 15). If a future time course experiment does not reveal significant autophagy signal, then this further supports the hypothesis that ATP release could have been induced through a pathway that is not autophagy-dependent [111].

Overall, the results of this assay suggest immunogenic, caspase-3 dependent apoptosis, marked by the Annexin V/PI assay results as well as ATP release and calreticulin exposure [12].

The results of the autophagy study – as well as the identification of apoptotic cell death and previous ATP study – also pose interesting further questions about the tunability of IL structure to modulate interactions with 4T1 cells. Future studies may investigate whether IL anion chain length impact ATP release, ATP release over time, and autophagy activation by investigating IL Panel 1 and additionally, an expanded panel of ILs with many different anion chain lengths, beyond six through ten. The complex interplay of IL-induced ATP release, caspase-dependent immunogenic apoptosis, and potential autophagy suppression is important because it can elucidate an IL's capacity for activating immunogenic cell death and also other anti-tumor activity that could be potentially ATP-limiting. The applications of these questions go beyond whole tumor cell vaccines towards using IL for anti-cancer uses more broadly [9], [69], [117].

6. Conclusion

This work has provided further characterization of the biological interface of ILs in activating tumor cell immunogenicity for whole tumor cell vaccines. Here, we highlight the importance of considering the structure of IL anions, which have previously been thought to be less deterministic of IL activity than the cation structure [11].

We found that IL-induced cytotoxicity increases with anion chain carbon length and with concentration, and that it decreases with adding branched methyl groups, ethyl groups, and double bonds in the anion structure. Tuning IL anions has been found to modulate ICD signals as well. Branching and unsaturation also decreases exposure of calreticulin, a main marker of ICD. Panel 2 ILs were shown to induce ATP release in a concentration-dependent manner, though the effect of branching and unsaturation on ATP release may require further investigation. Since 4T1

cells are known to be poorly immunogenic cancer cells, the display of strong ICD signals adds to the significance of using ILs for this function [31]. Moreover, ILs appear to activate apoptotic cell death over other cell death pathways, such as necrosis and necroptosis. Stage of apoptosis was found to be tunable, based on IL anion carbon chain length (Figure 7). The extent to which apoptotic cell death appears to generally decrease with anion branching and unsaturation in anions with the same number of carbons (Figure 8).

From our preliminary screen, ILs do not appear to significantly activate autophagy after 24 hours. However, ILs appear to induce ATP release, although when autophagy is inhibited, they do not induce ATP release. This phenomenon may be explored in more detail in future time course assays. Overall, cell death characterized by ATP release, caspase-3 dependent apoptotic behavior, and calreticulin exposure supports immunogenic apoptosis as the broad mechanism of cell death induced by IL panels [12].

Future works will seek to apply learnings from tuning IL-induced ICD and cell death to phagocytosis studies. These assays will include co-cultures of DCs and 4T1 cells to examine whether structural changes in IL anions (branching and unsaturation) affect the ability of DCs to uptake treated 4T1 cells. From there, tri-culture studies, including treated 4T1 cells, DCs, and T-cells, can examine the ability of APCs to stimulate T cells *in vitro*.

Continued studies can also directly compare the cytotoxicity, immunogenicity, and cell death pathways induced by our libraries of ILs to cell death that is induced by irradiation, a current common cell death strategy in whole tumor cell vaccines that is known to have insufficient

immunogenicity. Finally, ILs with branched and unsaturated anions can be included in *in vivo* studies in 4T1 mice. This current investigation's findings can support such *in vivo* studies and can aid in optimizing ILs used in preclinical treatments and contribute to understanding of outcomes, towards the goal of improving therapies for solid tumor patients.

References

[1] E. McGowan, Q. Lin, G. Ma, H. Yin, S. Chen, and Y. Lin, "PD-1 disrupted CAR-T cells in the treatment of solid tumors: Promises and challenges," *Biomed. Pharmacother.*, vol. 121, p. 109625, Jan. 2020, doi: 10.1016/j.biopha.2019.109625.

[2] P. Wu *et al.*, "Adaptive Mechanisms of Tumor Therapy Resistance Driven by Tumor Microenvironment," *Front. Cell Dev. Biol.*, vol. 9, p. 641469, Mar. 2021, doi: 10.3389/fcell.2021.641469.

[3] P. Guha, K. R. Heatherton, K. P. O'Connell, I. S. Alexander, and S. C. Katz, "Assessing the Future of Solid Tumor Immunotherapy," *Biomedicines*, vol. 10, no. 3, p. 655, Mar. 2022, doi: 10.3390/biomedicines10030655.

[4] J. Wu and D. J. Waxman, "Immunogenic chemotherapy: Dose and schedule dependence and combination with immunotherapy," *Cancer Lett.*, vol. 419, pp. 210–221, Apr. 2018, doi: 10.1016/j.canlet.2018.01.050.

[5] O. Kepp *et al.*, "Immunogenic cell death modalities and their impact on cancer treatment," *Apoptosis*, vol. 14, no. 4, pp. 364–375, Apr. 2009, doi: 10.1007/s10495-008-0303-9.

[6] D. L. Wagner *et al.*, "Immunogenicity of CAR T cells in cancer therapy," *Nat. Rev. Clin. Oncol.*, vol. 18, no. 6, pp. 379–393, Jun. 2021, doi: 10.1038/s41571-021-00476-2.

[7] L. Galluzzi *et al.*, "Molecular mechanisms of cell death: recommendations of the Nomenclature Committee on Cell Death 2018," *Cell Death Differ.*, vol. 25, no. 3, pp. 486–541, Mar. 2018, doi: 10.1038/s41418-017-0012-4.

[8] J. Fucikova *et al.*, "Detection of immunogenic cell death and its relevance for cancer therapy," *Cell Death Dis.*, vol. 11, no. 11, pp. 1–13, Nov. 2020, doi: 10.1038/s41419-020-03221-2.

[9] I. Ali, M. Hozaifa, S. Ali, A. Malik, and M. Locatelli, "Advances in ionic liquids as future anti-cancer drugs," *J. Mol. Liq.*, vol. 388, p. 122823, Oct. 2023, doi: 10.1016/j.molliq.2023.122823.

[10] B. Montico, A. Nigro, V. Casolaro, and J. Dal Col, "Immunogenic Apoptosis as a Novel Tool for Anticancer Vaccine Development," *Int. J. Mol. Sci.*, vol. 19, no. 2, p. 594, Feb. 2018, doi: 10.3390/ijms19020594.

[11] X.-Y. Li, C.-Q. Jing, W.-L. Lei, J. Li, and J.-J. Wang, "Apoptosis caused by imidazolium-based ionic liquids in PC12 cells," *Ecotoxicol. Environ. Saf.*, vol. 83, pp. 102–107, Sep. 2012, doi: 10.1016/j.ecoenv.2012.06.013.

[12] G. Gupta, K. Borglum, and H. Chen, "Immunogenic Cell Death: A Step Ahead of Autophagy in Cancer Therapy," *J. Cancer Immunol.*, vol. 3, no. 1, pp. 47–59, 2021, doi: 10.33696/cancerimmunol.3.041.

[13] Y. Zhang and Z. Zhang, "The history and advances in cancer immunotherapy: understanding the characteristics of tumor-infiltrating immune cells and their therapeutic implications," *Cell. Mol. Immunol.*, vol. 17, no. 8, pp. 807–821, Aug. 2020, doi: 10.1038/s41423-020-0488-6.

[14] D. T. Debela *et al.*, "New approaches and procedures for cancer treatment: Current perspectives," *SAGE Open Med.*, vol. 9, p. 20503121211034366, Aug. 2021, doi: 10.1177/20503121211034366.

[15] W. M. C. van den Boogaard, D. S. J. Komninos, and W. P. Vermeij, “Chemotherapy Side-Effects: Not All DNA Damage Is Equal,” *Cancers*, vol. 14, no. 3, p. 627, Jan. 2022, doi: 10.3390/cancers14030627.
[16] M. T. Amjad, A. Chidharla, and A. Kasi, “Cancer Chemotherapy,” in *StatPearls*, Treasure Island (FL): StatPearls Publishing, 2024. Accessed: Mar. 17, 2024. [Online]. Available: http://www.ncbi.nlm.nih.gov/books/NBK564367/
[17] O. Trédan, C. M. Galmarini, K. Patel, and I. F. Tannock, “Drug resistance and the solid tumor microenvironment,” *J. Natl. Cancer Inst.*, vol. 99, no. 19, pp. 1441–1454, Oct. 2007, doi: 10.1093/jnci/djm135.
[18] Q. Sun, Z. Hong, C. Zhang, L. Wang, Z. Han, and D. Ma, “Immune checkpoint therapy for solid tumours: clinical dilemmas and future trends,” *Signal Transduct. Target. Ther.*, vol. 8, no. 1, p. 320, Aug. 2023, doi: 10.1038/s41392-023-01522-4.
[19] S. Ghosh *et al.*, “Triple negative breast cancer and non-small cell lung cancer: Clinical challenges and nano-formulation approaches,” *J. Control. Release Off. J. Control. Release Soc.*, vol. 337, pp. 27–58, Sep. 2021, doi: 10.1016/j.jconrel.2021.07.014.
[20] S.-R. Niavarani *et al.*, “Heterologous prime-boost cellular vaccination induces potent antitumor immunity against triple negative breast cancer,” *Front. Immunol.*, vol. 14, p. 1098344, Feb. 2023, doi: 10.3389/fimmu.2023.1098344.
[21] Y. Liu *et al.*, “Advances in immunotherapy for triple-negative breast cancer,” *Mol. Cancer*, vol. 22, no. 1, p. 145, Sep. 2023, doi: 10.1186/s12943-023-01850-7.
[22] T. Li *et al.*, “Discrepant antitumor efficacies of three CpG oligodeoxynucleotide classes in monotherapy and co-therapy with PD-1 blockade,” *Pharmacol. Res.*, vol. 161, p. 105293, Nov. 2020, doi: 10.1016/j.phrs.2020.105293.
[23] M. Hosseini *et al.*, “Cancer Vaccines for Triple-Negative Breast Cancer: A Systematic Review,” *Vaccines*, vol. 11, no. 1, p. 146, Jan. 2023, doi: 10.3390/vaccines11010146.
[24] Washington University School of Medicine, “A Phase 1 Clinical Trial to Evaluate the Safety and Immunogenicity of a Personalized Synthetic Long Peptide Breast Cancer Vaccine Strategy in Patients With Persistent Triple-Negative Breast Cancer Following Neoadjuvant Chemotherapy,” clinicaltrials.gov, Clinical trial registration NCT02427581, Mar. 2022. Accessed: Dec. 31, 2023. [Online]. Available: https://clinicaltrials.gov/study/NCT02427581
[25] Washington University School of Medicine, “A Phase 1 Clinical Trial to Evaluate the Safety and Immunogenicity of a Personalized Polyepitope DNA Vaccine Strategy in Breast Cancer Patients With Persistent Triple-Negative Disease Following Neoadjuvant Chemotherapy,” clinicaltrials.gov, Clinical trial registration NCT02348320, Jun. 2020. Accessed: Dec. 31, 2023. [Online]. Available: https://clinicaltrials.gov/study/NCT02348320
[26] X. Zhang *et al.*, “Neoantigen DNA vaccines are safe, feasible, and capable of inducing neoantigen-specific immune responses in patients with triple negative breast cancer.” medRxiv, p. 2021.11.19.21266466, Nov. 21, 2021. doi: 10.1101/2021.11.19.21266466.
[27] BioNTech SE, “First-in-human Clinical Study With RNA-Immunotherapy Combination of IVAC_W_bre1_uID and IVAC_M_uID for Individualized Tumor Therapy in Triple Negative Breast Cancer Patients,” clinicaltrials.gov, Clinical trial registration NCT02316457, Jul. 2023. Accessed: Dec. 31, 2023. [Online]. Available: https://clinicaltrials.gov/study/NCT02316457
[28] M. Schmidt *et al.*, “88MO T-cell responses induced by an individualized neoantigen specific immune therapy in post (neo)adjuvant patients with triple negative breast cancer,” *Ann. Oncol.*, vol. 31, p. S276, Sep. 2020, doi: 10.1016/j.annonc.2020.08.209.

[29] "Mouse 4T1 Breast Tumor Model - Pulaski - 2000 - Current Protocols in Immunology - Wiley Online Library." Accessed: Mar. 17, 2024. [Online]. Available: https://currentprotocols.onlinelibrary.wiley.com/doi/10.1002/0471142735.im2002s39
[30] C. J. Aslakson and F. R. Miller, "Selective events in the metastatic process defined by analysis of the sequential dissemination of subpopulations of a mouse mammary tumor," *Cancer Res.*, vol. 52, no. 6, pp. 1399–1405, Mar. 1992.
[31] B. A. Pulaski and S. Ostrand-Rosenberg, "Reduction of established spontaneous mammary carcinoma metastases following immunotherapy with major histocompatibility complex class II and B7.1 cell-based tumor vaccines," *Cancer Res.*, vol. 58, no. 7, pp. 1486–1493, Apr. 1998.
[32] S. A. Sadeghi Najafabadi, A. Bolhassani, and M. R. Aghasadeghi, "Tumor cell-based vaccine: an effective strategy for eradication of cancer cells," *Immunotherapy*, vol. 14, no. 8, pp. 639–654, Jun. 2022, doi: 10.2217/imt-2022-0036.
[33] L. Diao and M. Liu, "Rethinking Antigen Source: Cancer Vaccines Based on Whole Tumor Cell/tissue Lysate or Whole Tumor Cell," *Adv. Sci.*, vol. 10, no. 22, p. 2300121, 2023, doi: 10.1002/advs.202300121.
[34] C. L.-L. Chiang, G. Coukos, and L. E. Kandalaft, "Whole Tumor Antigen Vaccines: Where Are We?," *Vaccines*, vol. 3, no. 2, pp. 344–372, Apr. 2015, doi: 10.3390/vaccines3020344.
[35] L. Menger *et al.*, "Cardiac glycosides exert anticancer effects by inducing immunogenic cell death," *Sci. Transl. Med.*, vol. 4, no. 143, p. 143ra99, Jul. 2012, doi: 10.1126/scitranslmed.3003807.
[36] G. Dranoff *et al.*, "Vaccination with irradiated tumor cells engineered to secrete murine granulocyte-macrophage colony-stimulating factor stimulates potent, specific, and long-lasting anti-tumor immunity," *Proc. Natl. Acad. Sci. U. S. A.*, vol. 90, no. 8, pp. 3539–3543, Apr. 1993, doi: 10.1073/pnas.90.8.3539.
[37] J. Guo *et al.*, "Cancer vaccines from cryogenically silicified tumour cells functionalized with pathogen-associated molecular patterns," *Nat. Biomed. Eng.*, vol. 6, no. 1, pp. 19–31, Jan. 2022, doi: 10.1038/s41551-021-00795-w.
[38] C. Seitz *et al.*, "Tumor Cell-Based Vaccine Generated With High Hydrostatic Pressure Synergizes With Radiotherapy by Generating a Favorable Anti-tumor Immune Microenvironment," *Front. Oncol.*, vol. 9, p. 805, 2019, doi: 10.3389/fonc.2019.00805.
[39] G. Kroemer, L. Galluzzi, O. Kepp, and L. Zitvogel, "Immunogenic cell death in cancer therapy," *Annu. Rev. Immunol.*, vol. 31, pp. 51–72, 2013, doi: 10.1146/annurev-immunol-032712-100008.
[40] A. Degterev and J. Yuan, "Expansion and evolution of cell death programmes," *Nat. Rev. Mol. Cell Biol.*, vol. 9, no. 5, pp. 378–390, May 2008, doi: 10.1038/nrm2393.
[41] J. Yuan and D. Ofengeim, "A guide to cell death pathways," *Nat. Rev. Mol. Cell Biol.*, pp. 1–17, Dec. 2023, doi: 10.1038/s41580-023-00689-6.
[42] M. S. D'Arcy, "Cell death: a review of the major forms of apoptosis, necrosis and autophagy," *Cell Biol. Int.*, vol. 43, no. 6, pp. 582–592, Jun. 2019, doi: 10.1002/cbin.11137.
[43] M. L. Coleman, E. A. Sahai, M. Yeo, M. Bosch, A. Dewar, and M. F. Olson, "Membrane blebbing during apoptosis results from caspase-mediated activation of ROCK I," *Nat. Cell Biol.*, vol. 3, no. 4, pp. 339–345, Apr. 2001, doi: 10.1038/35070009.
[44] N. Bata and N. D. P. Cosford, "Cell Survival and Cell Death at the Intersection of Autophagy and Apoptosis: Implications for Current and Future Cancer Therapeutics," *ACS Pharmacol. Transl. Sci.*, vol. 4, no. 6, pp. 1728–1746, Dec. 2021, doi: 10.1021/acsptsci.1c00130.

[45] I. Vitale *et al.*, “Apoptotic cell death in disease-Current understanding of the NCCD 2023,” *Cell Death Differ.*, vol. 30, no. 5, pp. 1097–1154, May 2023, doi: 10.1038/s41418-023-01153-w.
[46] D. R. Green, T. Ferguson, L. Zitvogel, and G. Kroemer, “Immunogenic and tolerogenic cell death,” *Nat. Rev. Immunol.*, vol. 9, no. 5, pp. 353–363, May 2009, doi: 10.1038/nri2545.
[47] I. Vermes, C. Haanen, H. Steffens-Nakken, and C. Reutellingsperger, “A novel assay for apoptosis Flow cytometric detection of phosphatidylserine expression on early apoptotic cells using fluorescein labelled Annexin V,” *J. Immunol. Methods*, vol. 184, no. 1, pp. 39–51, Jul. 1995, doi: 10.1016/0022-1759(95)00072-I.
[48] E. Brauchle, S. Thude, S. Y. Brucker, and K. Schenke-Layland, “Cell death stages in single apoptotic and necrotic cells monitored by Raman microspectroscopy,” *Sci. Rep.*, vol. 4, no. 1, p. 4698, Apr. 2014, doi: 10.1038/srep04698.
[49] F. K.-M. Chan, K. Moriwaki, and M. J. De Rosa, “Detection of Necrosis by Release of Lactate Dehydrogenase (LDH) Activity,” *Methods Mol. Biol. Clifton NJ*, vol. 979, pp. 65–70, 2013, doi: 10.1007/978-1-62703-290-2_7.
[50] Y. K. Dhuriya and D. Sharma, “Necroptosis: a regulated inflammatory mode of cell death,” *J. Neuroinflammation*, vol. 15, no. 1, p. 199, Jul. 2018, doi: 10.1186/s12974-018-1235-0.
[51] K. P. Kotredes and A. M. Gamero, “Interferons as Inducers of Apoptosis in Malignant Cells,” *J. Interferon Cytokine Res.*, vol. 33, no. 4, pp. 162–170, Apr. 2013, doi: 10.1089/jir.2012.0110.
[52] L. Seifert and G. Miller, “Molecular Pathways: The Necrosome – A Target for Cancer Therapy,” *Clin. Cancer Res. Off. J. Am. Assoc. Cancer Res.*, vol. 23, no. 5, pp. 1132–1136, Mar. 2017, doi: 10.1158/1078-0432.CCR-16-0968.
[53] “Differences of Key Proteins between Apoptosis and Necroptosis - PMC.” Accessed: Mar. 27, 2024. [Online]. Available: https://www.ncbi.nlm.nih.gov/pmc/articles/PMC8684821/
[54] D. Bergamaschi, A. Vossenkamper, W. Y. J. Lee, P. Wang, E. Bochukova, and G. Warnes, “Simultaneous polychromatic flow cytometric detection of multiple forms of regulated cell death,” *Apoptosis Int. J. Program. Cell Death*, vol. 24, no. 5–6, pp. 453–464, Jun. 2019, doi: 10.1007/s10495-019-01528-w.
[55] P. Vandenabeele, T. Vanden Berghe, and N. Festjens, “Caspase Inhibitors Promote Alternative Cell Death Pathways,” *Sci. STKE*, vol. 2006, no. 358, pp. pe44–pe44, Oct. 2006, doi: 10.1126/stke.3582006pe44.
[56] K. R. Parzych and D. J. Klionsky, “An Overview of Autophagy: Morphology, Mechanism, and Regulation,” *Antioxid. Redox Signal.*, vol. 20, no. 3, pp. 460–473, Jan. 2014, doi: 10.1089/ars.2013.5371.
[57] “Flow Cytometric Analysis of Autophagic Activity with Cyto-ID Staining in Primary Cells.” Accessed: Mar. 23, 2024. [Online]. Available: https://bio-protocol.org/en/bpdetail?id=1090&type=0#.U2lDjUrD-Uk
[58] M. Su, Y. Mei, and S. Sinha, “Role of the Crosstalk between Autophagy and Apoptosis in Cancer,” *J. Oncol.*, vol. 2013, p. 102735, 2013, doi: 10.1155/2013/102735.
[59] Y.-J. Fan and W.-X. Zong, “The cellular decision between apoptosis and autophagy,” *Chin. J. Cancer*, vol. 32, no. 3, pp. 121–129, Mar. 2013, doi: 10.5732/cjc.012.10106.
[60] M. Michaud *et al.*, “Autophagy-dependent anticancer immune responses induced by chemotherapeutic agents in mice,” *Science*, vol. 334, no. 6062, pp. 1573–1577, Dec. 2011, doi: 10.1126/science.1208347.

[61] Y. Chu *et al.*, “Regulation of Autophagy by Glycolysis in Cancer,” *Cancer Manag. Res.*, vol. 12, pp. 13259–13271, Dec. 2020, doi: 10.2147/CMAR.S279672.
[62] “Introduction: Ionic Liquids | Chemical Reviews.” Accessed: Mar. 25, 2024. [Online]. Available: https://pubs.acs.org/doi/10.1021/acs.chemrev.7b00246
[63] A. M. Curreri, S. Mitragotri, and E. E. L. Tanner, “Recent Advances in Ionic Liquids in Biomedicine,” *Adv. Sci. Weinh. Baden-Wurtt. Ger.*, vol. 8, no. 17, p. e2004819, Sep. 2021, doi: 10.1002/advs.202004819.
[64] Md. K. Ali, R. M. Moshikur, R. Wakabayashi, M. Moniruzzaman, N. Kamiya, and M. Goto, “Biocompatible Ionic Liquid Surfactant-Based Microemulsion as a Potential Carrier for Sparingly Soluble Drugs,” *ACS Sustain. Chem. Eng.*, vol. 8, no. 16, pp. 6263–6272, Apr. 2020, doi: 10.1021/acssuschemeng.9b07773.
[65] M. Nurunnabi, K. N. Ibsen, E. E. L. Tanner, and S. Mitragotri, “Oral ionic liquid for the treatment of diet-induced obesity,” *Proc. Natl. Acad. Sci. U. S. A.*, vol. 116, no. 50, pp. 25042–25047, Dec. 2019, doi: 10.1073/pnas.1914426116.
[66] P. Kumari, V. V. S. Pillai, and A. Benedetto, “Mechanisms of action of ionic liquids on living cells: the state of the art,” *Biophys. Rev.*, vol. 12, no. 5, pp. 1187–1215, Sep. 2020, doi: 10.1007/s12551-020-00754-w.
[67] M. L. Stromyer *et al.*, “Synthesis, characterization, and biological activity of a triphenylphosphonium-containing imidazolium salt against select bladder cancer cell lines,” *Eur. J. Med. Chem.*, vol. 185, p. 111832, Jan. 2020, doi: 10.1016/j.ejmech.2019.111832.
[68] J. Huang *et al.*, “An Ionic Liquid Ablation Agent for Local Ablation and Immune Activation in Pancreatic Cancer,” *Adv. Sci.*, vol. 10, no. 10, p. 2206756, Jan. 2023, doi: 10.1002/advs.202206756.
[69] H. Albadawi *et al.*, “Percutaneous liquid ablation agent for tumor treatment and drug delivery,” *Sci. Transl. Med.*, vol. 13, no. 580, p. eabe3889, Feb. 2021, doi: 10.1126/scitranslmed.abe3889.
[70] N. Gal, D. Malferarri, S. Kolusheva, P. Galletti, E. Tagliavini, and R. Jelinek, “Membrane interactions of ionic liquids: Possible determinants for biological activity and toxicity,” *Biochim. Biophys. Acta BBA - Biomembr.*, vol. 1818, no. 12, pp. 2967–2974, Dec. 2012, doi: 10.1016/j.bbamem.2012.07.025.
[71] M. Musiał *et al.*, “Cytotoxicity of Ionic Liquids on Normal Human Dermal Fibroblasts in the Context of Their Present and Future Applications,” *ACS Sustain. Chem. Eng.*, vol. 9, no. 22, pp. 7649–7657, Jun. 2021, doi: 10.1021/acssuschemeng.1c02277.
[72] M. Petkovic *et al.*, “Novel biocompatible cholinium-based ionic liquids—toxicity and biodegradability,” *Green Chem.*, vol. 12, no. 4, pp. 643–649, Apr. 2010, doi: 10.1039/B922247B.
[73] C. M. Chism *et al.*, “Antimicrobial Effects of Anion Manipulation with Biocompatible Choline Carboxylic Acid-Based Ionic Liquids,” *ACS Appl. Eng. Mater.*, vol. 1, no. 1, pp. 23–31, Jan. 2023, doi: 10.1021/acsaenm.2c00004.
[74] F.-A. Farrugia and A. Charalampopoulos, “Pheochromocytoma,” *Endocr. Regul.*, vol. 53, no. 3, pp. 191–212, Jul. 2019.
[75] V. Tsarpali and S. Dailianis, “[omim][BF4]-mediated toxicity in mussel hemocytes includes its interaction with cellular membrane proteins,” *Aquat. Toxicol. Amst. Neth.*, vol. 203, pp. 88–94, Oct. 2018, doi: 10.1016/j.aquatox.2018.08.004.
[76] L.-X. Hu, Q. Xiong, W.-J. Shi, G.-Y. Huang, Y.-S. Liu, and G.-G. Ying, “New insight into the negative impact of imidazolium-based ionic liquid [C10mim]Cl on Hela cells: From

membrane damage to biochemical alterations," *Ecotoxicol. Environ. Saf.*, vol. 208, p. 111629, Jan. 2021, doi: 10.1016/j.ecoenv.2020.111629.
[77] S. Stolte *et al.*, "Effects of different head groups and functionalised side chains on the aquatic toxicity of ionic liquids," *Green Chem.*, vol. 9, no. 11, pp. 1170–1179, Oct. 2007, doi: 10.1039/B711119C.
[78] M. Vraneš *et al.*, "Correlation between lipophilicity of newly synthesized ionic liquids and selected Fusarium genus growth rate," *RSC Adv.*, vol. 9, no. 33, pp. 19189–19196, Jun. 2019, doi: 10.1039/C9RA02521A.
[79] PubChem, "trans-2-Octenoic acid." Accessed: Mar. 25, 2024. [Online]. Available: https://pubchem.ncbi.nlm.nih.gov/compound/5282714
[80] PubChem, "2,2-Dimethylhexanoic acid." Accessed: Mar. 25, 2024. [Online]. Available: https://pubchem.ncbi.nlm.nih.gov/compound/163217
[81] PubChem, "Octanoic Acid." Accessed: Mar. 25, 2024. [Online]. Available: https://pubchem.ncbi.nlm.nih.gov/compound/379
[82] PubChem, "2-Ethylhexanoic acid." Accessed: Mar. 25, 2024. [Online]. Available: https://pubchem.ncbi.nlm.nih.gov/compound/8697
[83] "Dead Cell Apoptosis Kits with Annexin V for Flow Cytometry." Accessed: Mar. 30, 2024. [Online]. Available: https://www.thermofisher.com/order/catalog/product/V13242
[84] "CyQUANT™ LDH Cytotoxicity Assay." Accessed: Mar. 25, 2024. [Online]. Available: https://www.thermofisher.com/order/catalog/product/C20300
[85] "ATP Determination Kit".
[86] PubChem, "Caproic Acid." Accessed: Mar. 25, 2024. [Online]. Available: https://pubchem.ncbi.nlm.nih.gov/compound/8892
[87] PubChem, "Hazardous Substances Data Bank (HSDB) : 6813." Accessed: Mar. 25, 2024. [Online]. Available: https://pubchem.ncbi.nlm.nih.gov/source/hsdb/6813
[88] PubChem, "Heptanoic Acid." Accessed: Mar. 25, 2024. [Online]. Available: https://pubchem.ncbi.nlm.nih.gov/compound/8094
[89] PubChem, "Hazardous Substances Data Bank (HSDB) : 5546." Accessed: Mar. 25, 2024. [Online]. Available: https://pubchem.ncbi.nlm.nih.gov/source/hsdb/5546
[90] "Caprylic acid." Accessed: Mar. 25, 2024. [Online]. Available: https://go.drugbank.com/drugs/DB04519
[91] PubChem, "Capric Acid." Accessed: Mar. 25, 2024. [Online]. Available: https://pubchem.ncbi.nlm.nih.gov/compound/2969
[92] "Capric acid." Accessed: Mar. 25, 2024. [Online]. Available: https://go.drugbank.com/drugs/DB03600
[93] L. Guha, T. Seenivasagan, S. T. Iqbal, O. P. Agrawal, and B. D. Parashar, "Behavioral and electrophysiological responses of Aedes albopictus to certain acids and alcohols present in human skin emanations," *Parasitol. Res.*, vol. 113, no. 10, pp. 3781–3787, Oct. 2014, doi: 10.1007/s00436-014-4044-0.
[94] R. C. Brands, M. J. J. Scheurer, S. Hartmann, A. Seher, A. C. Kübler, and U. D. A. Müller-Richter, "Apoptosis-sensitizing activity of birinapant in head and neck squamous cell carcinoma cell lines," *Oncol. Lett.*, vol. 15, no. 3, pp. 4010–4016, Mar. 2018, doi: 10.3892/ol.2018.7783.
[95] E. Eskandari and C. J. Eaves, "Paradoxical roles of caspase-3 in regulating cell survival, proliferation, and tumorigenesis," *J. Cell Biol.*, vol. 221, no. 6, p. e202201159, May 2022, doi: 10.1083/jcb.202201159.

[96] S. Stolte *et al.*, “Anion effects on the cytotoxicity of ionic liquids,” *Green Chem.*, vol. 8, no. 7, pp. 621–629, Jul. 2006, doi: 10.1039/B602161A.
[97] I. Martins *et al.*, “Molecular mechanisms of ATP secretion during immunogenic cell death,” *Cell Death Differ.*, vol. 21, no. 1, pp. 79–91, Jan. 2014, doi: 10.1038/cdd.2013.75.
[98] J. Mandl, T. Mészáros, G. Bánhegyi, and M. Csala, “Minireview: endoplasmic reticulum stress: control in protein, lipid, and signal homeostasis,” *Mol. Endocrinol. Baltim. Md*, vol. 27, no. 3, pp. 384–393, Mar. 2013, doi: 10.1210/me.2012-1317.
[99] A. Brusic *et al.*, “Detecting T-cell reactivity to whole cell vaccines,” *Oncoimmunology*, vol. 1, no. 7, pp. 1095–1103, Oct. 2012, doi: 10.4161/onci.20954.
[100] K. Seaver, O. Kourko, K. Gee, P. A. Greer, and S. Basta, “IL-27 Improves Prophylactic Protection Provided by a Dead Tumor Cell Vaccine in a Mouse Melanoma Model,” *Front. Immunol.*, vol. 13, p. 884827, Apr. 2022, doi: 10.3389/fimmu.2022.884827.
[101] W. Fang *et al.*, “Harnessing enucleated cancer cells as Trojan horse cell vaccines,” *Cell Rep. Phys. Sci.*, vol. 5, no. 1, p. 101752, Jan. 2024, doi: 10.1016/j.xcrp.2023.101752.
[102] J. Zhou, G. Wang, Y. Chen, H. Wang, Y. Hua, and Z. Cai, “Immunogenic cell death in cancer therapy: Present and emerging inducers,” *J. Cell. Mol. Med.*, vol. 23, no. 8, pp. 4854–4865, Aug. 2019, doi: 10.1111/jcmm.14356.
[103] C. L.-L. Chiang, F. Benencia, and G. Coukos, “Whole Tumor Antigen Vaccines,” *Semin. Immunol.*, vol. 22, no. 3, pp. 132–143, Jun. 2010, doi: 10.1016/j.smim.2010.02.004.
[104] R. Spisek *et al.*, “Induction of Leukemia-specific Cytotoxic Response by Cross-Presentation of Late-Apoptotic Leukemic Blasts by Autologous Dendritic Cells of Nonleukemic Origin1,” *Cancer Res.*, vol. 62, no. 10, pp. 2861–2868, May 2002.
[105] N. Khalid and M. Azimpouran, “Necrosis,” in *StatPearls*, Treasure Island (FL): StatPearls Publishing, 2024. Accessed: Mar. 23, 2024. [Online]. Available: http://www.ncbi.nlm.nih.gov/books/NBK557627/
[106] B. Yoo *et al.*, “Molecular mechanisms of ionic liquid cytotoxicity probed by an integrated experimental and computational approach,” *Sci. Rep.*, vol. 6, no. 1, p. 19889, Feb. 2016, doi: 10.1038/srep19889.
[107] K. Bakshi *et al.*, “Imidazolium-based ionic liquids cause mammalian cell death due to modulated structures and dynamics of cellular membrane,” *Biochim. Biophys. Acta BBA - Biomembr.*, vol. 1862, no. 2, p. 183103, Feb. 2020, doi: 10.1016/j.bbamem.2019.183103.
[108] S. R. Scheffer *et al.*, “Apoptotic, but not necrotic, tumor cell vaccines induce a potent immune response in vivo,” *Int. J. Cancer*, vol. 103, no. 2, pp. 205–211, Jan. 2003, doi: 10.1002/ijc.10777.
[109] K. Eloranta *et al.*, “Chloroquine Triggers Cell Death and Inhibits PARPs in Cell Models of Aggressive Hepatoblastoma,” *Front. Oncol.*, vol. 10, p. 1138, Jul. 2020, doi: 10.3389/fonc.2020.01138.
[110] Z. Zhang *et al.*, “Rapamycin maintains NAD^+/NADH redox homeostasis in muscle cells,” *Aging*, vol. 12, no. 18, pp. 17786–17799, Sep. 2020, doi: 10.18632/aging.103954.
[111] M. Dosch, J. Gerber, F. Jebbawi, and G. Beldi, “Mechanisms of ATP Release by Inflammatory Cells,” *Int. J. Mol. Sci.*, vol. 19, no. 4, Art. no. 4, Apr. 2018, doi: 10.3390/ijms19041222.
[112] PubChem, “Geranic acid.” Accessed: Mar. 22, 2024. [Online]. Available: https://pubchem.ncbi.nlm.nih.gov/compound/5275520

[113] X.-Y. Zhang *et al.*, “Hexokinase 2 confers resistance to cisplatin in ovarian cancer cells by enhancing cisplatin-induced autophagy,” *Int. J. Biochem. Cell Biol.*, vol. 95, pp. 9–16, Feb. 2018, doi: 10.1016/j.biocel.2017.12.010.
[114] Y.-J. Li *et al.*, “Autophagy and multidrug resistance in cancer,” *Chin. J. Cancer*, vol. 36, p. 52, Jun. 2017, doi: 10.1186/s40880-017-0219-2.
[115] G. Kroemer, C. Galassi, L. Zitvogel, and L. Galluzzi, “Immunogenic cell stress and death,” *Nat. Immunol.*, vol. 23, no. 4, pp. 487–500, Apr. 2022, doi: 10.1038/s41590-022-01132-2.
[116] N. Chen and V. Karantza-Wadsworth, “Role and regulation of autophagy in cancer,” *Biochim. Biophys. Acta BBA - Mol. Cell Res.*, vol. 1793, no. 9, pp. 1516–1523, Sep. 2009, doi: 10.1016/j.bbamcr.2008.12.013.
[117] T.-H. Han *et al.*, “Cancer-specific cytotoxicity of pyridinium-based ionic liquids by regulating hypoxia-inducible factor-1α-centric cancer metabolism,” *Ecotoxicol. Environ. Saf.*, vol. 248, p. 114334, Dec. 2022, doi: 10.1016/j.ecoenv.2022.114334.